Naval Research Laboratory

Washington, DC 20375-5320

NRL/MR/6180--12-9429

A Versatile Impactor-Inspired Sample Chamber with a Virtual Pin-Grid Array for Sensor Performance Evaluation

Christopher R. Field
Susan L. Rose-Pehrsson

Navy Technology Center for Safety and Survivability
Chemistry Division

Cy R. Tamanaha

Surface Nanoscience and Sensor Technology
Chemistry Division

Michael P. Malito

Nova Research, Inc.
Alexandria, Virginia

September 28, 2012

Approved for public release; distribution is unlimited.

REPORT DOCUMENTATION PAGE

Form Approved
OMB No. 0704-0188

Public reporting burden for this collection of information is estimated to average 1 hour per response, including the time for reviewing instructions, searching existing data sources, gathering and maintaining the data needed, and completing and reviewing this collection of information. Send comments regarding this burden estimate or any other aspect of this collection of information, including suggestions for reducing this burden to Department of Defense, Washington Headquarters Services, Directorate for Information Operations and Reports (0704-0188), 1215 Jefferson Davis Highway, Suite 1204, Arlington, VA 22202-4302. Respondents should be aware that notwithstanding any other provision of law, no person shall be subject to any penalty for failing to comply with a collection of information if it does not display a currently valid OMB control number. **PLEASE DO NOT RETURN YOUR FORM TO THE ABOVE ADDRESS.**

1. REPORT DATE *(DD-MM-YYYY)*
28-09-2012

2. REPORT TYPE
Memorandum Report

3. DATES COVERED *(From - To)*
November 2011 – May 2012

4. TITLE AND SUBTITLE

A Versatile Impactor-Inspired Sample Chamber with a Virtual Pin-Grid Array for Sensor Performance Evaluation

5a. CONTRACT NUMBER

5b. GRANT NUMBER

5c. PROGRAM ELEMENT NUMBER

5d. PROJECT NUMBER

5e. TASK NUMBER

5f. WORK UNIT NUMBER
61-8906-P-1-5, 61-8906-M-1-5

6. AUTHOR(S)

Christopher R. Field, Susan L. Rose-Pehrsson, Cy R. Tamanaha, and Michael P. Malito*

7. PERFORMING ORGANIZATION NAME(S) AND ADDRESS(ES)

Naval Research Laboratory
4555 Overlook Avenue, SW
Washington, DC 20375-5320

8. PERFORMING ORGANIZATION REPORT NUMBER

NRL/MR/6180--12-9429

9. SPONSORING / MONITORING AGENCY NAME(S) AND ADDRESS(ES)

Department of Homeland Security (DHS)
Science and Technology Directorate
245 Murray Lane
Washington, DC 20528-0206

10. SPONSOR / MONITOR'S ACRONYM(S)

DHS

11. SPONSOR / MONITOR'S REPORT NUMBER(S)

12. DISTRIBUTION / AVAILABILITY STATEMENT

Approved for public release; distribution is unlimited.

13. SUPPLEMENTARY NOTES

*Nova Research, Inc., 1900 Elkin Street, Suite 230, Alexandria, VA 22308

14. ABSTRACT

An impactor-inspired sample chamber was constructed and assembled to evaluate sensor performance during exposure to trace analytes, such as explosives and chemical warfare agents. A flexible, virtual pin-grid array (PGA) was created with a series of hardware and software to make electrical connections without need to create prototype, expensive circuits. The sample chamber and Virtual-PGA electronics were characterized and tested using a thermal imager and a custom temperature and relative humidity sensor. The chamber and electronics are capable of evaluating sensor performance under a variety of environmental conditions and analytes.

15. SUBJECT TERMS

Sample chamber
Impactor
Virtual pin grid array
Sensor evaluation

16. SECURITY CLASSIFICATION OF:			17. LIMITATION OF ABSTRACT	18. NUMBER OF PAGES	19a. NAME OF RESPONSIBLE PERSON
					Christopher R. Field
a. REPORT	b. ABSTRACT	c. THIS PAGE	Unlimited	34	19b. TELEPHONE NUMBER *(include area code)*
Unclassified	Unclassified	Unclassified	Unclassified		(202) 404-3365

Standard Form 298 (Rev. 8-98)
Prescribed by ANSI Std. Z39.18

TABLE OF CONTENTS

I. Introduction 1

II. Sample Chamber 3

III. Electronics 7

IV. Software 10

V. Characterization 14

VI. Conclusions 18

Appendix A: Circuit Diagrams for the Virtual Pin-Grid Array 21

Appendix B: A Custom Temperature and Relative Humidity Sensor 24

Appendix C: The Computer-Aided Design (CAD) files for the Impactor Sample Chamber 30

Appendix D: Source code for the Virtual-PGA and Data Acquisition Software 31

I. Introduction

A variety of electrical-based sensors are being developed to detect a wide range of gaseous analytes, such as volatile organic compounds (VOCs), explosives, toxic industrial compounds (TICs), and chemical warfare agents [1–6]. These sensors often utilize novel materials and nanostructures like single-walled carbon nanotubes, graphene, or micro-cantilevers to convert chemical interactions into electrical signal [7–11]. The majority of sensor research is conducted by individual groups working to demonstrate a proof-of-principle for a material or sensing mechanism. A vast array of prototype sensors has been fabricated and each new sensor leads to unique packaging, electronics, and vapor delivery systems. The packaging must be designed to minimize dead volume, rapidly deliver vapor to the sensor, and minimize wall adsorption effects. The electronics must be low noise, easily fabricated, and ultimately connected to a computer for data logging. The vapor delivery component must be capable of delivering a wide range of analytes under various environmental conditions, such as temperature and humidity, in order to thoroughly test and characterize sensors. All of these components contribute to sensor performance, and all of these components are prototypes themselves. Therefore, it is difficult to compare the performance of these new and novel sensors. To "standardize" the testing process, the Naval Research Laboratory (NRL) undertook the design, assembly, and successful testing of a unique **T**race **Ex**plosives **T**estbed (TExT) system to deliver known quantities of explosive vapors to prototype sensors and commercialized instrumentation. The TExT can be easily extended to generate and deliver vapor streams of interferents, VOCs, TICs, and chemical warfare agents.

A design challenge was to uniformly transport these generated vapors to a multitude of sensors that could potentially possess any number of physical and electronic configurations. The variability in packaging and size makes designing and fabricating a universal testing platform difficult. Sensors can be housed in off-the-shelf ceramic or plastic chip carriers typically used in the semiconductor industry, or they can be mounted in custom packages that include a fluidic microchannel and related plumbing [11,12]. In the simplest form, sensors can be mounted on a stage with probes. In addition, the sizes of the sensors range from the nano-scale to the macro-scale, and each prototype may use a different transduction mechanism that requires monitoring different electrical properties—voltage, current, resistance, frequency, or capacitance—to detect vapors.

Prior to designing our new sensor testing platform, each sensor was accompanied by a dedicated prototype circuit to monitor electrical response. An example of such a circuit board is seen in Figure 1.

Manuscript approved July 30, 2012

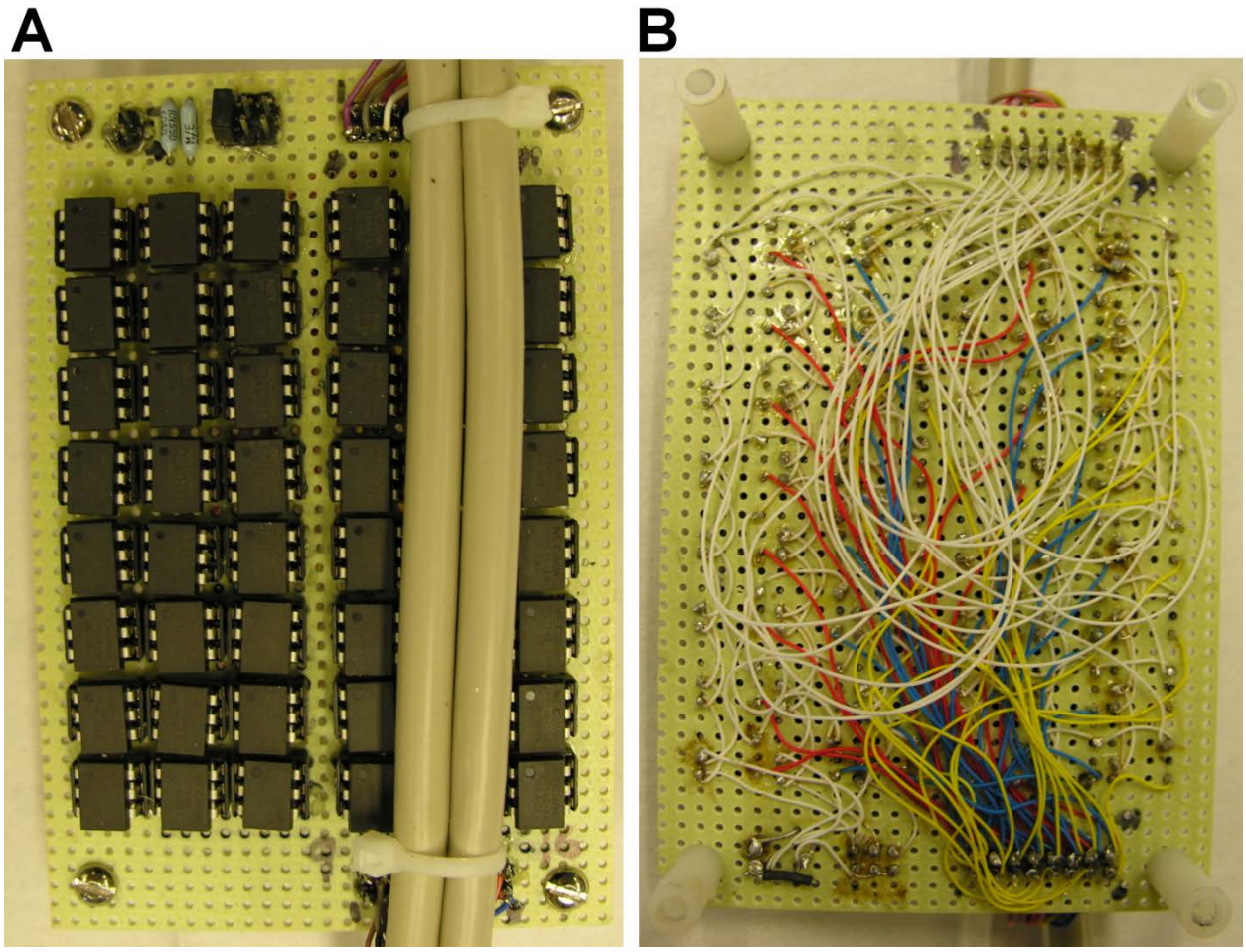

Figure 1: An example prototype circuit board constructed for sensor performance evaluation with (A) the top view and (B) the bottom view. The 6-pin dual in-line package relays are used to route four channels to a single sensor. The wiring and soldering of the prototype circuit is laborious and time consuming.

The 6-pin dual in-line package (DIP) relays were used to route four sensor channels to eight pins of a prototype sensor. The complexity of even a simple circuit for sensor response testing is clearly demonstrated in the wiring seen in Figure 1B. Furthermore, a single sensor chip may actually be an array of sensors requiring scalable electronics to monitor the response of each sensor in the array simultaneously. The routing of single and multiple sensor channels to electrical measurement instrumentation is laborious and time consuming. Each new sensor circuit ultimately requires specific, custom software and computer communication to record and plot data. Therefore, it would be advantageous to have an electrical system capable of re-configuring, re-routing, and scaling sensor channels without having to make a new circuit and write custom software for every sensor. Thus, a universal and easily adaptable sensor testing platform was needed that could accommodate the wide range of possible sensor configurations.

Herein, an impactor-inspired sample chamber with a novel electrical system is described, which is capable of delivering a wide variety of vapors to prototype sensors without the need for creating new packaging, circuits, or software. The sample chamber focuses on off-the-shelf parts to minimize cost and manufacturing time while maximizing flexibility. A uniform vapor

front is evenly distributed across the surface of a sensor while a Virtual Pin-Grid Array (VPGA) routes sensor channels to electrical measurement instrumentation. The majority of sensor literature focuses on the sensor. Instead, our focus was on the design and usability of a flexible, universal sensor testing system with an impactor-inspired sample chamber and VPGA.

II. Sample Chamber

The impactor-inspired sample chamber was designed to disseminate a uniform vapor front normal to, and evenly distributed across, the surface of a sensor being tested. A concept drawing of the sample chamber is seen in Figure 2A, while a computer-aided design (CAD) drawing of the actual sample chamber is seen in Figure 2B.

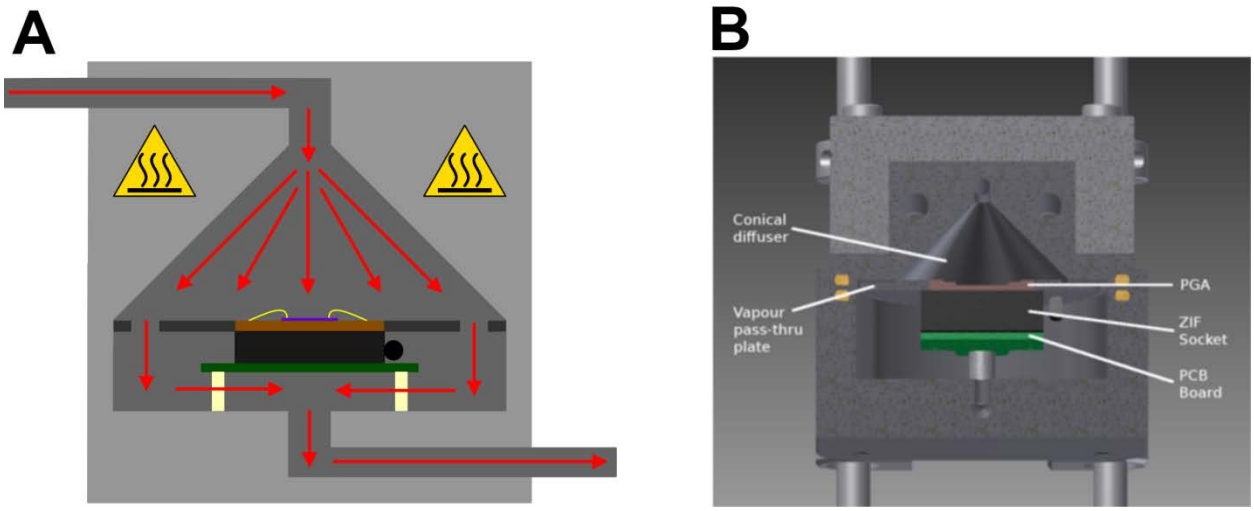

Figure 2: (A) A concept drawing of the impactor-inspired sample chamber and (B) a computer-aided design drawing of the actual sample chamber. The red arrows indicate the desired flow path for the analyte through the chamber.

The basic design uses a cone-shaped diffuser geometry to facilitate the uniform delivery of vapor to a sensor positioned at the center of a vapor pass-thru plate. Vapor flows from the cone housed in the top half to the bottom half, where the sensor is mounted in the center. The top section has provisions to secure two cartridge heaters (CH13696, Tutco, Cookeville, Tennessee USA) for heating the walls of the cone diffuser, which is necessary to minimize wall adsorption effects of semi-volatile compounds. The red arrows in Figure 2A indicate a general flow path of the vapor as it enters and exits the sample chamber. The cone-shaped geometry, along with a high impedance exit slit leading to the thirty-six exit holes that circumscribe the interior of the sample chamber was modeled in FEMLAB to verify the vapor flow. Figure 3 shows the results of a finite-element analysis simulation of vapor entering and exiting the sample chamber at a flow rate of 60 mL min^{-1}. The results in Figure 3 are comparable to the desired flow path through the chamber indicated by the red arrows in the concept drawing of Figure 2A. The vapor pass-thru plate helps generate a uniform vapor concentration across the entire surface area of the PGA and shields the mounting electronics from analyte vapors.

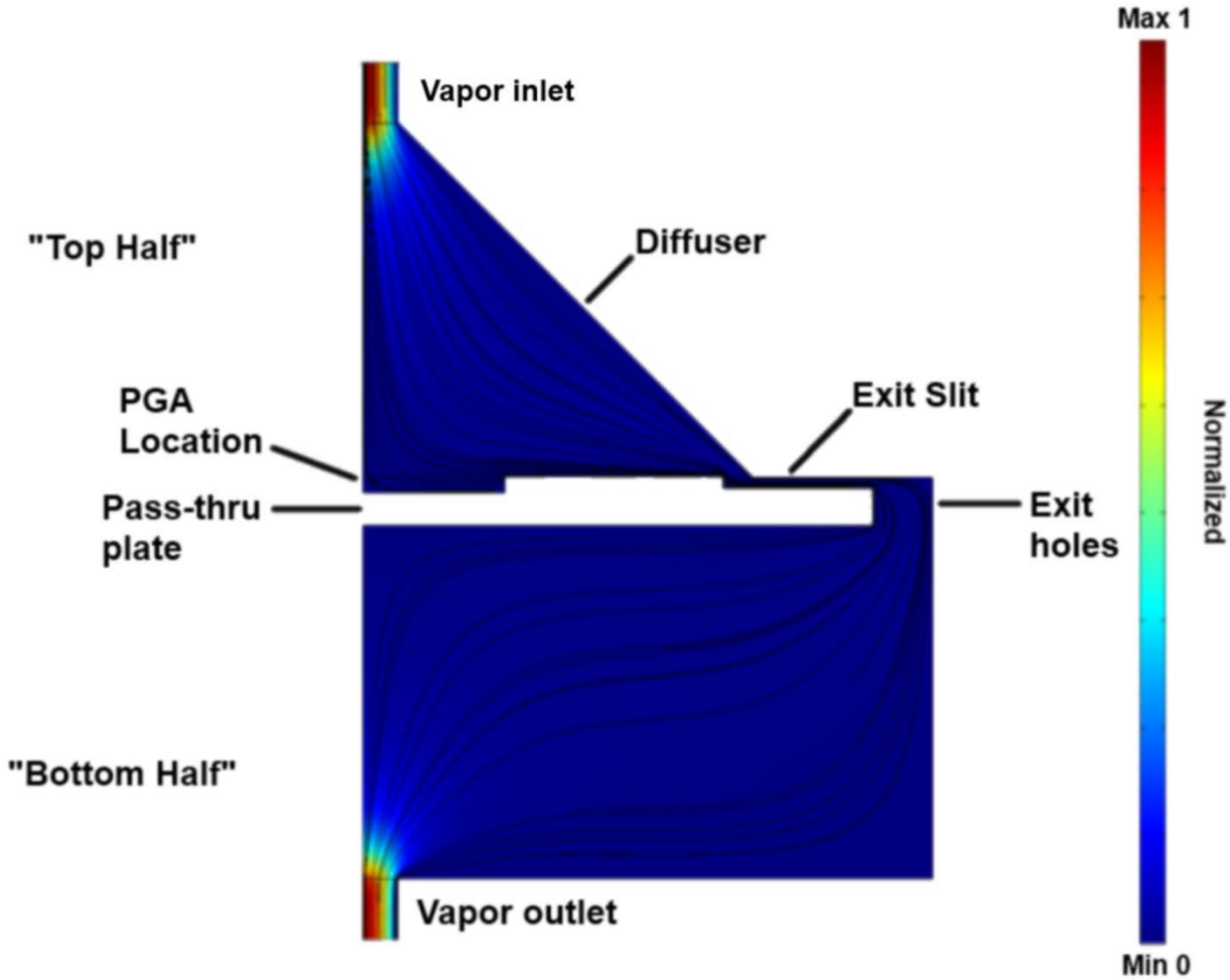

Figure 3: The finite-element analysis model of the vapor flow plotted as streamlines and velocity contours within the impactor-inspired sample chamber. The chamber is symmetric along the vertical axis. The flow rate has been normalized for comparison.

The sample chamber is divided into top and bottom halves, and each half is seen in the cross section of the assembled sample chamber in Figure 2B. The top and bottom halves were fabricated from 316-stainless steel. The steel was then polished and coated with a silionization process (SilcoNert, SilcoTek, Bellefonte, Pennsylvania USA) to reduce wall adsorption effects. The top half consists of two parts, where the inner part was made of silionized-coated stainless steel and the outer housing was made of aluminum, as indicated by the two different gray-colored regions in Figure 2B. The two parts of the top section were designed to focus the heat to the inner walls of the cone geometry, reduce weight, and minimize cost. Any surface in contact with the vapor stream, regardless if it is the top or bottom section, is silionized stainless steel with the exception of the sensor mounting components.

The bottom half of the sample chamber consists of a metal housing made of silionized stainless steel and the sensor mounting components. Prior to loading a sensor into the chamber, a sensor is mounted on a PGA chip carrier (CPG06402, Spectrum Semiconductor Materials, San Jose, California USA). Conductive epoxy, or double sided tape, can be used for mounting and electrical connections from chip to carrier are made *via* wire bonding. The PGA

used in this setup has one of the largest cavity sizes commercially available at approximately 1 cm^2. The PGA is inserted into a zero-insertion force (ZIF, 200-6310-9UN-1900, 3M, St. Paul, Minnesota USA) socket with a printed circuit board (PCB) for wiring the pins to external electronics. The ZIF is positioned such that the PGA is in the center of the cone of the top section of the sample chamber. Figure 4A shows an image of the ZIF socket, PCB, and PGA in the bottom half of the chamber. The entire ZIF socket assembly can be removed for sensors larger than the PGA or to mount alterative socket configurations.

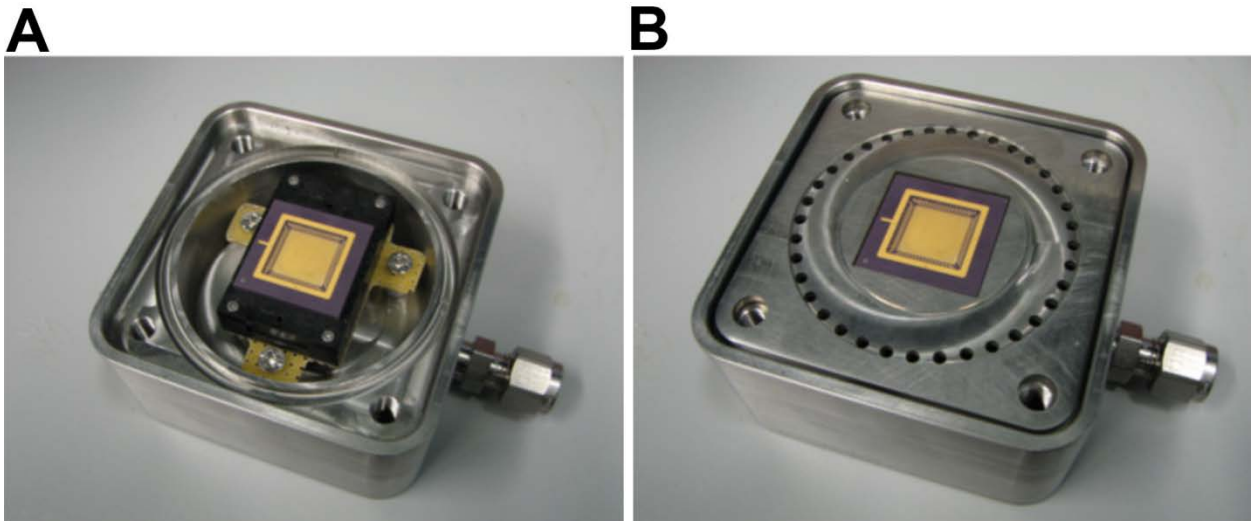

Figure 4: Close up of the bottom half of the chamber. These photos were taken prior to the silionization treatment of the stainless steel components. (A) The mounted circuit board with the ZIF socket and PGA packaging. (B) The placement of the vapor pass-thru plate when the top half mates with the bottom half.

The ZIF socket, circuit board, and wires of the bottom section was not treated or coated to reduce analyte adsorption. Instead, a silionized stainless steel vapor pass-thru plate with a square hole in the center for the PGA and a ring of holes along the outside perimeter was placed over top of the socket, circuit board, and wires. There is no seal around the PGA with the pass-thru plate to facilitate ease of loading and unloading chips. Figure 4B shows an image of the vapor pass-thru plate prior to application of the silionization coating. The vapor flows down from the top section, interacts with the sensor in the center, and is swept out of the chamber by the ring of exhaust ports in the vapor pass-thru plate. Analytes can still adsorb onto the electrical components, but the vapor pass-thru plate ensures this occurs downstream from the sensor.

A ¼-in. silionized tube connector (SS-400-1-2W, Swagelok, Cleveland, Ohio USA) has been welded to the top and bottom sections for fluid connections. Vapor streams can either be pumped (pushed) or pulled through the sample chamber depending on the requirements of the sensor performance evaluation. For most applications, a mass flow controller (M100 Smart-Trak 2, Sierra Instruments, Monterey, California USA) capable of operating at a pressure differential of 15 psi, ca. 1 atm, was used in combination with a vacuum pump to pull analyte through the sample chamber. The cone geometry yields a total chamber volume of 8.36 mL above the sensor. A relatively low volume is typically desired to minimize deleterious flow dynamics, wall

effects, and improve sensor response time; however, sample chamber volume has been designed for flexibility to accommodate a variety of different sized sensors.

The top section can be heated to 130°C, while the bottom section is not actively heated. The cartridge heaters can be used to reduce analyte adsorption onto the walls of the cone geometry or to conduct temperature performance studies of prototype sensors. Holes were drilled around the cone for cartridge heaters and are seen in Figure 2B. The top section temperature is monitored with a thermocouple (HTTC36-K-18G-1.25, Omega Engineering, Bridgeport, New Jersey, USA) and regulated with a Proportional-Integral-Differential (PID) temperature controller (CSi32, Omega Engineering, Bridgeport, New Jersey USA).

The entire chamber was mounted on two parallel rails. While the top section was fixed to the rails, the chamber's bottom section has linear bearings (LHSSK8, MiSUMi, Schaumburg, Illinois USA) which allow it to smoothly ride on the rails upon separation from the top section. This configuration aids in rapid sensor loading and unloading from the chamber and interfacing with a variety of vapor delivery systems. A base has also been constructed for mounting to an optics breadboard. The rail-mounted configuration with the sample chamber opened for sensor loading and unloading is seen in Figure 5. Springs were mounted on the rails to prevent damage to the relatively heavy bottom section during sensor loading and unloading. The complete computer-aided design (CAD) files for the impactor-inspired sample chamber can be found in Appendix C.

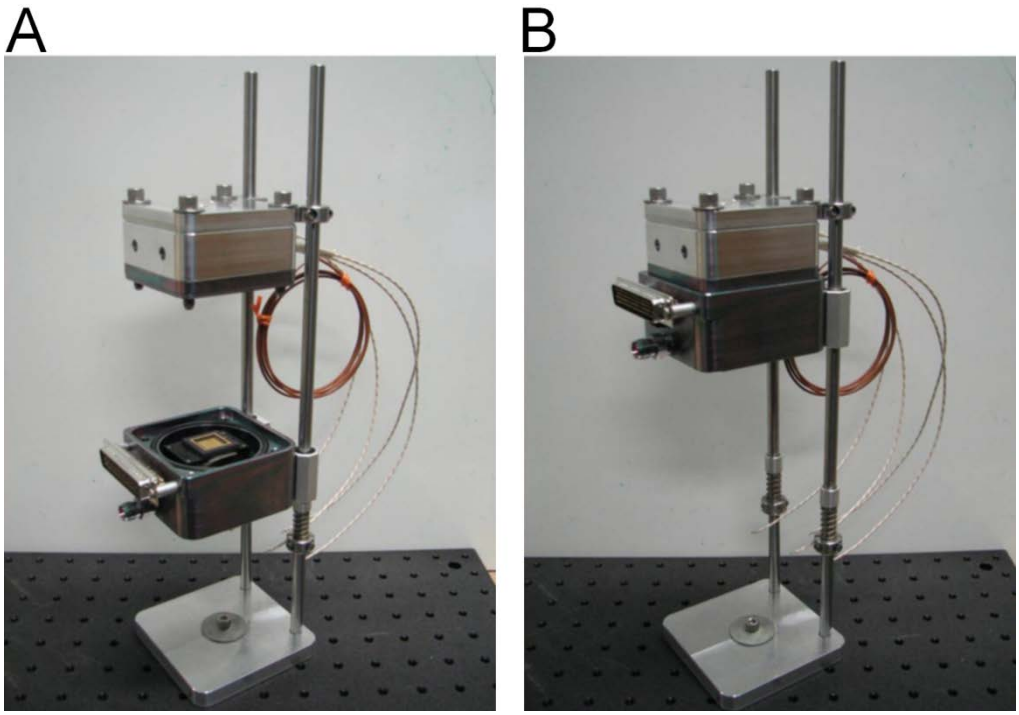

Figure 5: The impactor-inspired sample chamber on rails for easy loading and unloading for PGA-mounted sensors. (A) The top and bottom halves of the sample chamber separated for loading and unloading of the sensors. (B) The top and bottom halves of the chamber closed together and ready for vapor delivery. Any surface in contact with the analyte vapor is treated with the silionization process. The untreated portions are aluminum to minimize weight, reduce cost, and focus the heat to the walls to minimize wall-adsorption effects.

III. Electronics

The PGA used for mounting sensors in the sample chamber has sixty-four individually addressable pins. To manage all possible pin configurations to electrical measurement instrumentation, a VPGA was created using a 64x4 switch matrix (40-500-001, Pickering, Essex United Kingdom), a simple connection box, and an in-house written LabVIEW program. Figure 6 shows a diagram of the components that make up the VPGA.

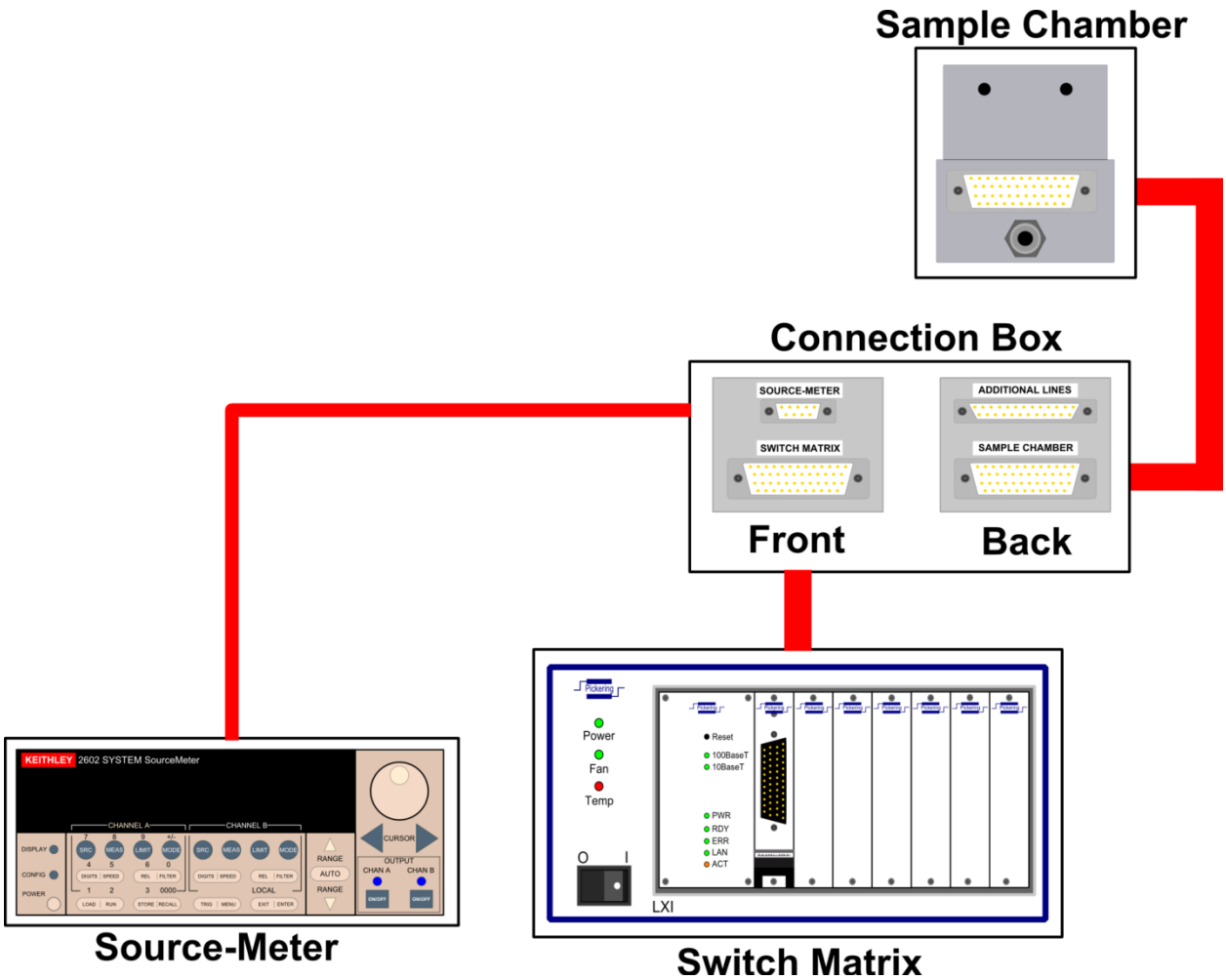

Figure 6: A single chamber configuration of the Virtual-PGA. A source-meter is connected to a 64x4 switch matrix through a connection box. The four channels from the source-meter are routed through the switch matrix to the sixty-four pins of the PGA housed in the sample chamber. The red lines indicate the cable connections between the various components.

A source-meter (2602, Keithley, Cleveland, Ohio USA) was used to supply either a constant voltage or current and measure current, voltage, resistance, or power. The source-meter is used as an example in this article but can easily be replaced with different electrical measurement instrumentation, such as an oscilloscope, lock-in amplifier, or semiconductor parameter analyzer depending on the application and sensor transduction mechanism. The source-meter has two independent units (Channel A and Channel B) with four channels per

unit, yielding a total of eight channels. Each unit is capable of sourcing or measuring a voltage or current up to 40 V or 2 A, respectively. Additionally, the source-meter has fourteen digital input/output (DIO) channels that can be accessed by a 25-pin D-sub connector (DB25) mounted on the back panel.

Only one unit is used in the configuration in Figure 6 for simplicity. The four channels of the source-meter are *source high*, *source low*, *sense high*, and *sense low*. All four channels are necessary for 4-wire resistance measurements but only *source high* and *source low* are used for 2-wire measurements. The four channels are connected to a connection box through a 9-pin male D-sub connector (DB9). Only four of the nine pins of the DB9 connector are used, which allows the addition of the second unit of the source-meter to be connected to the system in future applications. A circuit diagram for the connection box can be found in Appendix A.

The 64x4 switch matrix was connected to the system through a 78-pin male high density D-sub connector (DB78) mounted on the connection box of Figure 6. The four output channels were connected in the connection box to the four inputs, or *Y,* channels of the 64x4 switch matrix. The sixty-four output, or *X*, channels of the switch matrix were connected to another male DB78 connector and ultimately connected to a male DB78 connector mounted externally on the sample chamber. Each *X* channel was connected to a pin in the ZIF socket of the sample chamber with a simple PCB. All 78 channels of the DB78 connector on the sample chamber were passed through to the interior of the chamber, but only the first sixty-four, which correspond to the *X* channels of the switch matrix, were soldered to the ZIF socket. The remaining fourteen channels were left as wire leads for future applications. The pins of the PGA were routed to the external DB78 connector to match the pin outs of the 64x4 switch matrix. Appendix A shows a circuit diagram for the PGA and external DB78 connector. Non-magnetic, polyimide-coated copper wire was used for wiring inside the chamber and the through-hole was sealed with silicone. A circuit diagram summarizing the electrical connections for the complete VPGA system can be found in Appendix A.

The electronics are capable of scaling to seven sample chambers with the addition of a multiplexer. The 64x4 switch matrix is a PXI board and was housed in a LXI chassis (60-102-001, Pickering, Essex United Kingdom) with a switching speed of less than 400 µs for AC or DC signals up to 60 V and 2 A. The chassis has seven slots and can accommodate any PXI compatible board. Thus, seven 64x4 switch matrix boards can be loaded into the chassis and the source-meter routed through a multiplexer (7001 chassis and 7011 board, Keithley, Cleveland, Ohio USA) as diagramed in Figure 7.

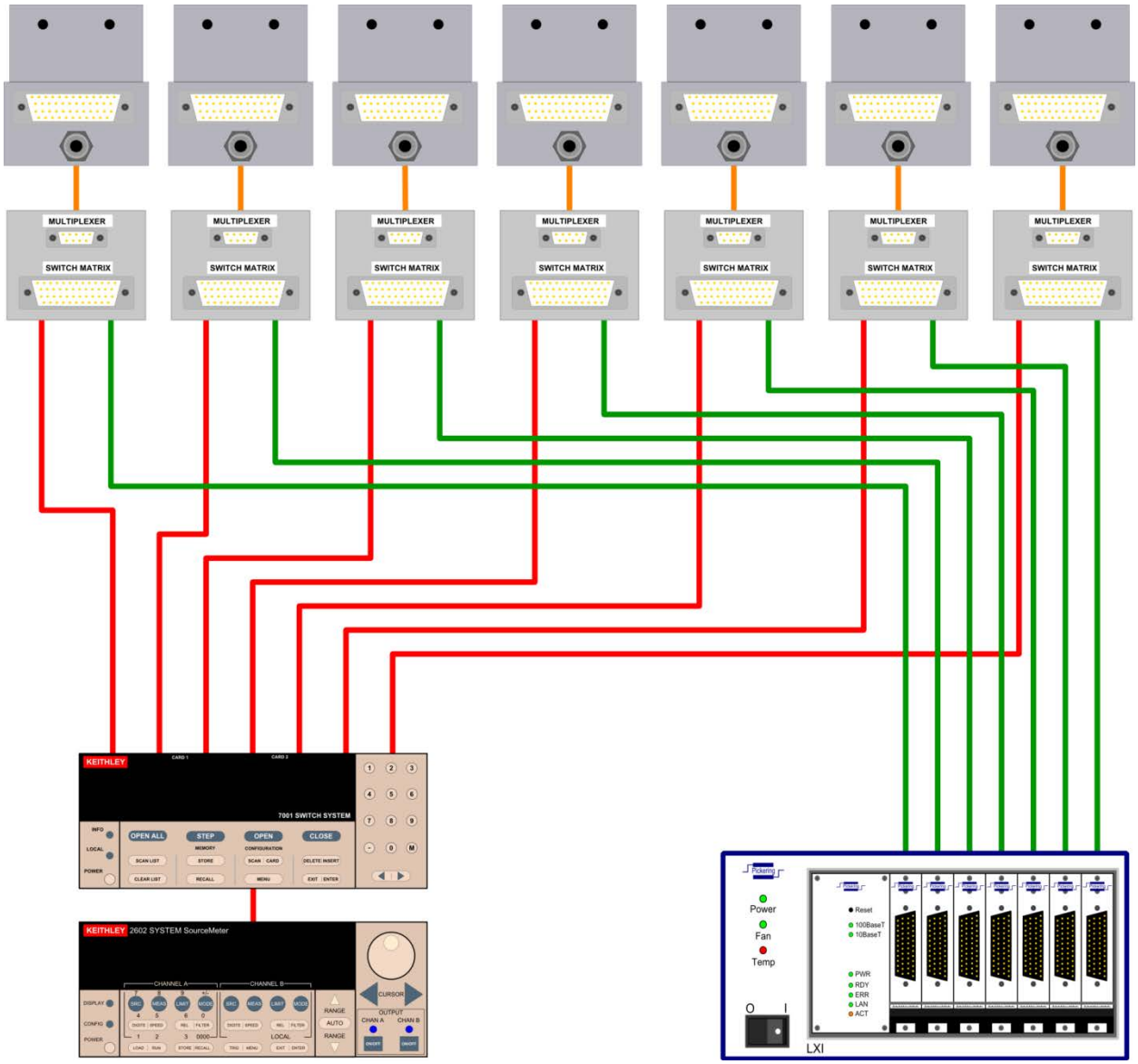

Figure 7: The Virtual-PGA electronics scaled to seven sample chambers with the inclusion of a multiplexer. The red lines indicate the electrical connections for the four channels from the source-meter. The green lines indicate the electrical connections between the sixty-four channels of the switch matrix and the connection box. The orange lines indicate the connection between the sample chamber and the 78-pin D-sub connector on the back side of the connection box.

The source-meter could be connected to the multiplexer and the multiplexer connected to each of the DB9 connectors of the connection boxes. The multiplexer is a 10x4 switch capable of both AC and DC signals, and the four channels of a single unit in the source-meter can be routed up to ten different channels at an actuation speed of 3 ms. Two 10x4 switch boards can be connected to the chassis of the multiplexer, where the second board would be used for the second source-meter unit (Channel B) in future applications. The multiplexer negates the need for additional source-meters and simplifies the data collection. For a typical seven chamber experiment, the pin patterns of the PGAs for each of the seven sample chambers are selected through the switch matrices in the LXI chassis while the multiplexer rapidly scans through the

sample chambers with the source-meter recording data. In theory, if a sensor were an array of sixty-four sensors with each channel on the PGA connected to a sensor, then in a seven sample chamber configuration, 448 sensors could be monitored simultaneously with the configuration outlined in Figure 7.

IV. Software

The electronics are controlled by a centralized program written in LabVIEW. The LXI chassis communicates *via* TCP/IP over a local area network connection. The source-meter and multiplexer communicate *via* a General Purpose Interface Bus (GPIB) connection and a USB-to-GPIB adaptor (GPIB-USB-HS, National Instruments, Austin, Texas USA). The interface of the software is an image of the PGA, where each pin has one of four buttons to turn on or off. The four buttons correspond to the four *Y* channels of the 64x4 switch matrix. Figure 8 shows a side-by-side comparison of the hardware PGA to the software PGA.

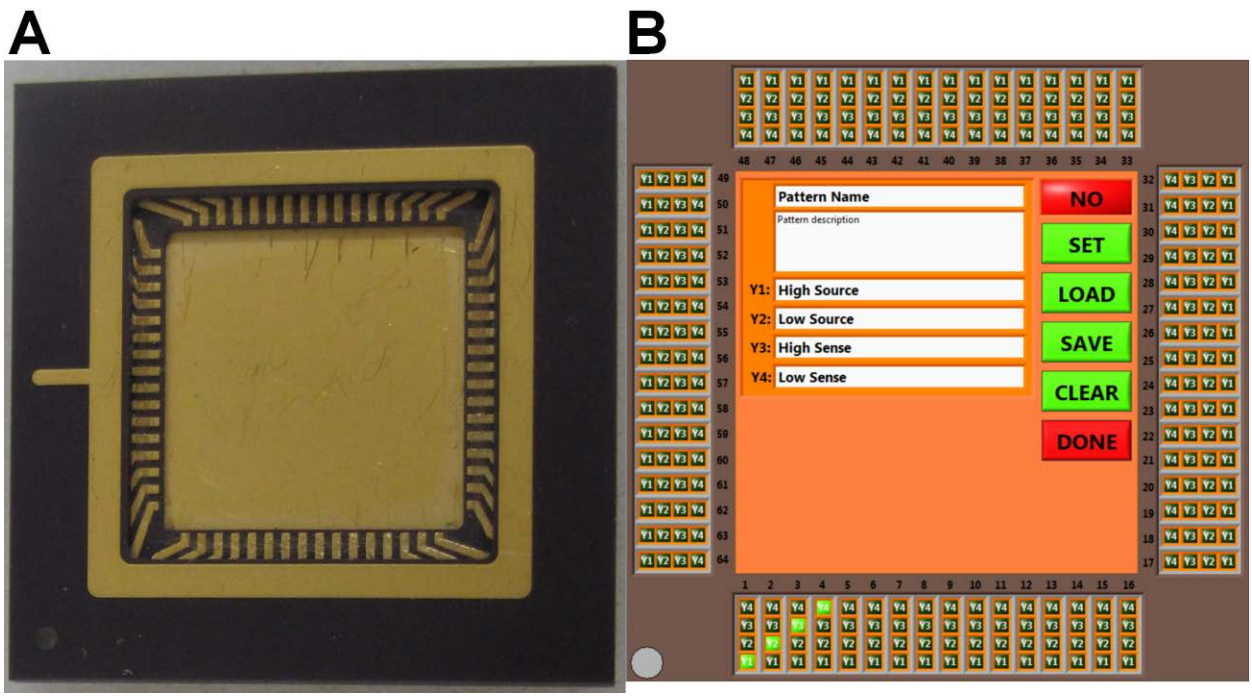

Figure 8: (A) A physical pin-grid array with sixty-four individually addressable pins. The circle in the lower left-hand corner indicates the location of the first pin. (B) The Virtual-PGA software interface, where the circle in the lower left-hand corner mimics the Pin 1 position indicator on the physical PGA. The green lights indicate those pins are connected to either Y_1, Y_2, Y_3, or Y_4 channels. The pattern of selected pins can be named with additional information and the *Y* channels can be labeled with more descriptive names.

The *Y* channels can be renamed with more descriptive labels using the text inputs in the center of the software PGA. The pin selection, or pattern, can also be given a name for quick identification with additional supporting information listed in the description field. The user can simply click on any of the sixty-four pins around the PGA to make a connection to any of the four *Y* channels of the switch matrix and ultimately the source-meter. The VPGA software is

written as both a stand-alone application and as a library to be embedded or extended in other programs (see Appendix D).

Pin selections and labels are saved in an e**X**tensible **M**arkup **L**anugage (XML) file. XML files can be created with any text editor. The software is capable of saving current pin configurations and loading previous ones from the XML files. The pin selections can also be made in the XML file prior to starting the software. The ability to create pin selection files without the VPGA software improves usability and interpretability with other data acquisition systems and software. Table 1 shows a list of the XML tags used to define a pin selection configuration along with a brief description of each tag, and Figure 9 shows an example text file using the XML tags from Table 1.

Table 1: A summary of the elements that make up the XML file format of the VPGA interface.

Tag	Attributes	Description
switch	None	The root element of the XML file
description	None	Information about the switch and pattern
sequence	None	Reserved for future use
pattern	Name	The pin selection of PGA pins to source-meter functions
Y1	Label	The Y_1 channel of the switch matrix
Y2	Label	The Y_2 channel of the switch matrix
Y3	Label	The Y_3 channel of the switch matrix
Y4	Label	The Y_4 channel of the switch matrix
pin	Id	The physical PGA pin

```xml
<?xml version="1.0" encoding="UTF-8"?>
<switch>
    <description>
        SHT15 temperature and relative humidity sensor mountd on a PCB the same size as a PGA.
        The sensor hub is v2.0.0 in the white box with removable front and back panels.
    </description>
    <sequence>
        <pattern name="Temp and RH Sensor">
            <Y1 label="GND">
                <pin id="3"/>
            </Y1>
            <Y2 label="DATA">
                <pin id="35"/>
            </Y2>
            <Y3 label="VDD">
                <pin id="19"/>
            </Y3>
            <Y4 label="CLK">
                <pin id="51"/>
            </Y4>
        </pattern>
    </sequence>
</switch>
```

Figure 9: An example pin configuration saved in a text file using the XML tags from Table 1. A custom temperature and relative humidity sensor with four pin connections (GND, DATA, VDD, and CLK) is used as an example sensor.

The root element of the XML file is the *switch* tag, which contains a *description* and a *sequence* element. The *description* tag is additional information about the pin selection. The *sequence* tag is currently not used, but is included for future applications where the pattern must be changed in a set sequence, or series, and allows for multiple pin selections to be cycled during data acquisition. The actual pin selections are defined in the *pattern* tag, which contains four tags for the four *Y* channels (Y_1, Y_2, Y_3, and Y_4) of the switch matrix and a *label* attribute. Each *Y* channel tag has child elements that correspond to the pins on the physical PGA. Multiple pins can be listed for each *Y* channel, where the *id* attribute indicates the physical PGA pin. An example XML file and schema are provided in Appendix D along with the complete LabVIEW software. The software provided in Appendix D is capable of creating, saving, and loading patterns for a single sample chamber, but it has not been expanded to multiple chambers for use in the configuration seen in Figure 7. Future versions of the software and the XML file definition will be extended to the seven sample chamber configuration.

The VPGA software is integrated with the sample chamber control and monitoring software. An example of the interface for the sample chamber control software is seen in Figure 10. The sample chamber and associated components, VPGA, temperature controller, and mass flow controller, are represented as images in the interface. Each image can be selected to activate a pop-up dialog to set the electrical connections, temperature, and flow rate, respectively. The image of the sample chamber can be selected to display a file selection dialog, where a configuration file specific to the chamber can be selected. The configuration file contains the electrical connections, ports, and default settings for each of the components associated with the chamber.

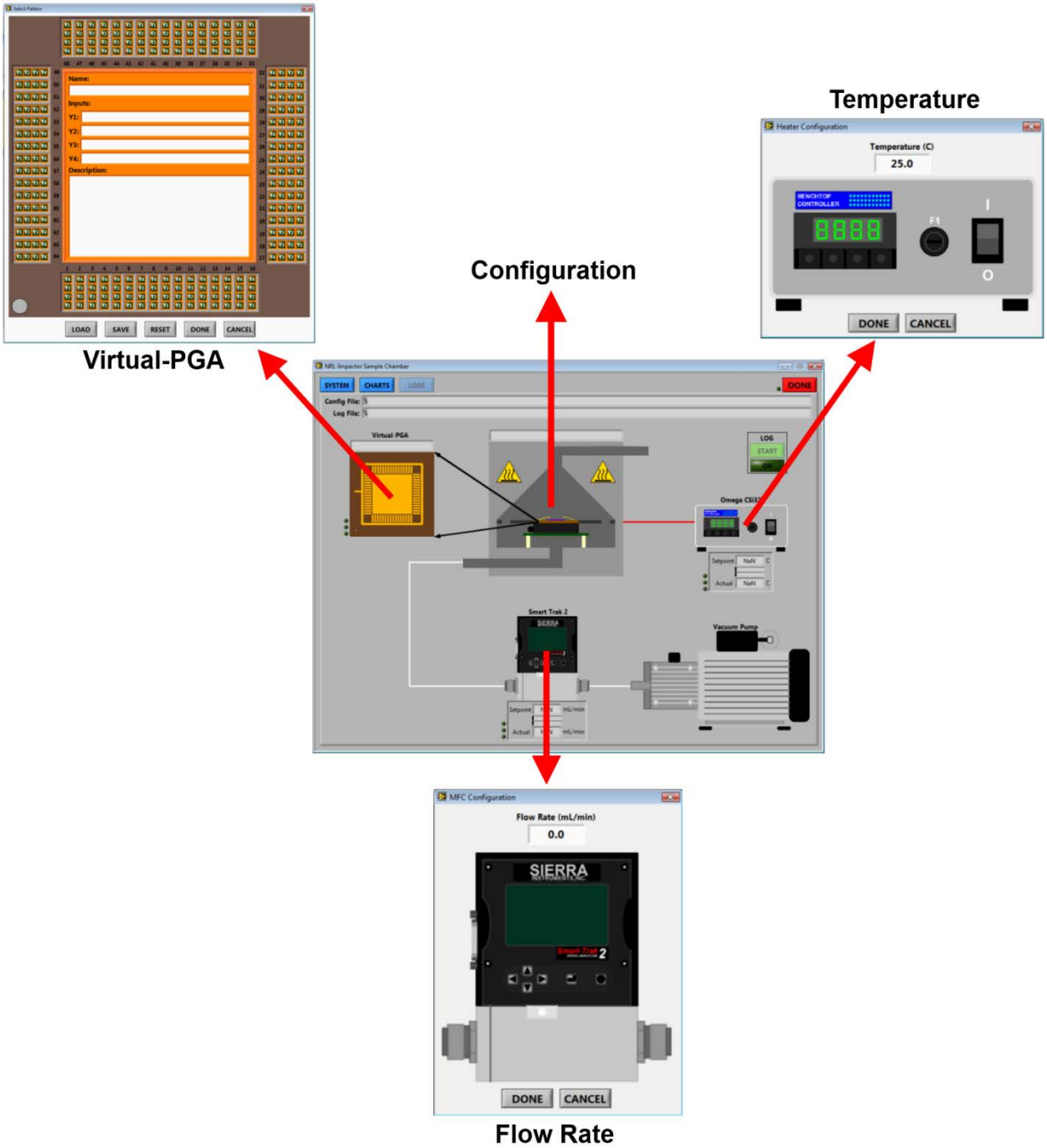

Figure 10: A diagram of the interface for controlling and monitoring the sample chamber. The interface includes a variety of pop-up dialogs for selecting the PGA connections, temperature, and flow rate, respectively. Additionally, a configuration file for the sample chamber can be selected and loaded by clicking on the image of the chamber in the interface.

The temperature and flow rate, both set point and actual, are logged to a comma-separated file that is organized by year, month, and day. The values are logged to the file every second (sample rate of 1 Hz). The most recent values are displayed in a plot versus time on another screen of the interface (not shown). The plot versus time provides a graphical representation of

the performance of the sample chamber during sensor evaluation. Furthermore, the log files can be loaded and displayed in the software through another screen in the interface (not shown) to evaluate the performance of the chamber after sensor evaluation. The log is created automatically upon loading a configuration file, but a manual control is provided for the user. The log file is named with a timestamp to easily locate the conditions during sensor evaluation.

V. Characterization

The sample chamber was characterized using a thermal imager (Ti55FT, Fluke, Everett, Washington USA) and a custom temperature and relative humidity sensor designed to be inserted into the ZIF socket of the VPGA hardware. The details of the temperature and relative humidity sensor can be found in Appendix B. Initially, the sample chamber temperature was ramped from 25°C to 130°C at room temperature (25°C) without air flow through the sample chamber, i.e. the mass flow controller flow rate was 0 mL min^{-1}. Figure 11 shows the thermal images during the ramping of the sample chamber temperature.

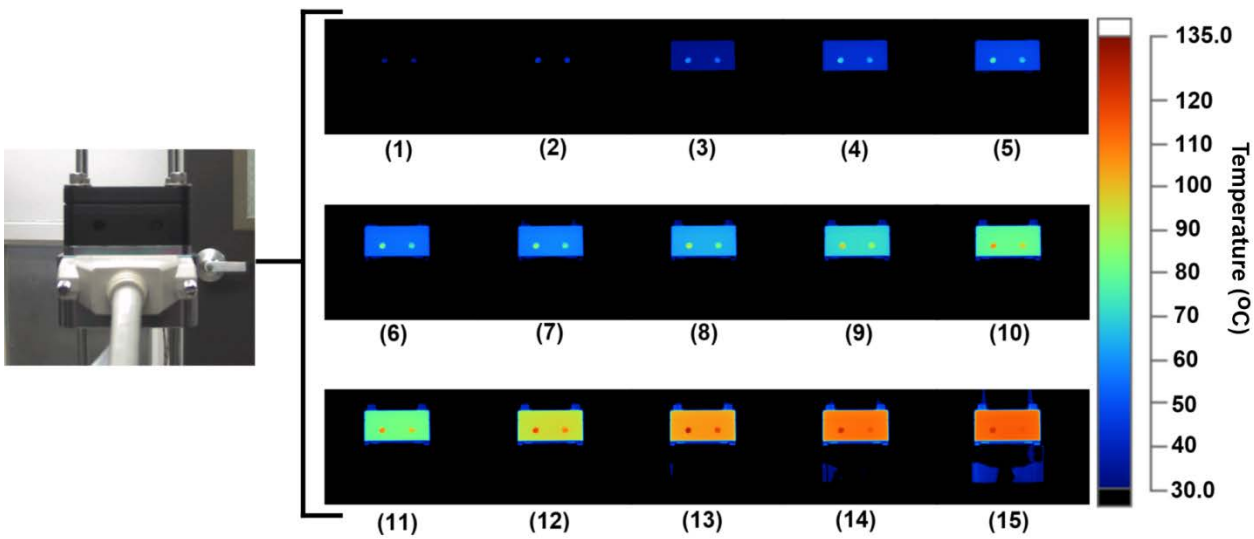

Figure 11: Thermal images of the outside of the sample chamber acquired while increasing the chamber temperature from 25°C to 130°C without air flow. The air flow was set to 0.0 mL min^{-1} to establish a baseline and determine the uniformity of the heating through the top and bottom sections of the chamber. The inset on the left shows the visible image of the sample chamber for reference of the thermal images. The emissivity was 0.95.

In each thermal image, the two circles are the cartridge heaters straddling the cone inside the sample chamber. The heat radiates from the heaters and is fairly uniform as the temperature reaches 130°C. As expected, the overall sample chamber temperature follows the cartridge heater temperature. The insert on the left in Figure 11 shows the visible image of the sample chamber, where the thermal images were recorded viewing the electronics connector and exit port for the air flow.

Additionally, the heat does not appear to effectively transfer from the top section to the bottom section. This is further demonstrated by the thermal images in Figure 12, which were recorded once the sample chamber reached 130°C. The heating was fairly uniform over the entire top section of the sample chamber.

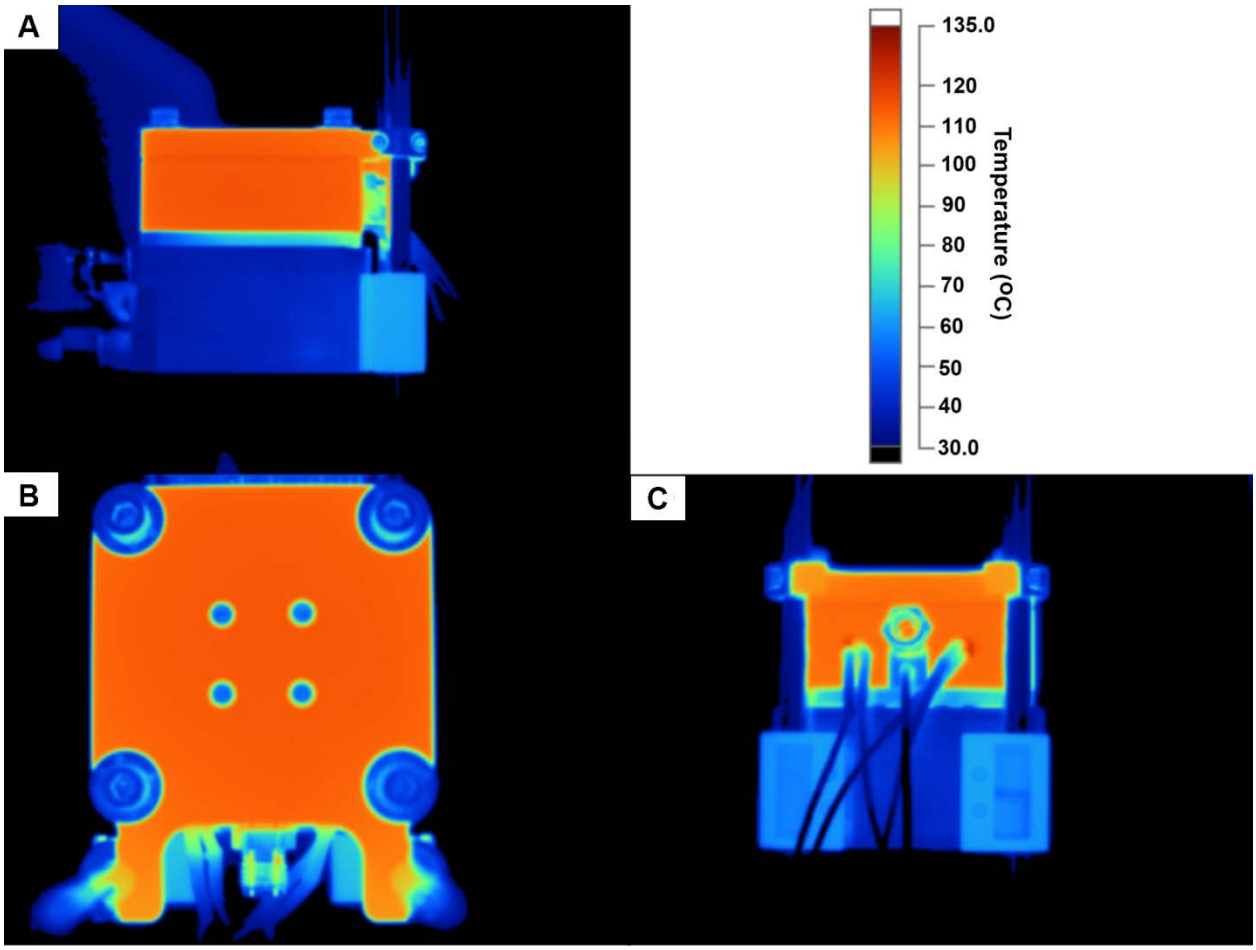

Figure 12: Thermal images of the (A) side, (B) top, and (C) back of the sample chamber after the temperature has equilibrated at 130°C without air flow. The emissivity was 0.95. The temperature is uniform throughout the top section, but some heat is transferred to the support rods *via* the clamp of the top section.

However, heat does flow to the support and guide rails that allow for easier loading and unloading of sensors. The top section is in thermal contact with the support rods through the clamps and aluminum cover. The heat does not appear to transfer to the bottom section through the linear bearings, but the linear bearings did heat to approximately 60°C at a chamber temperature of 130°C. The results from Figure 11 and Figure 12 indicate the heating of the sample chamber occurs uniformly, thus ultimately reducing wall adsorption effects of analyte vapor streams. Furthermore, the bottom section, which houses the sensor, was relatively cooler than the top section, allowing sensor temperature to be independently regulated separately from the sample chamber wall temperature.

The internal temperature of the sample chamber was recorded using a custom temperature and relative humidity sensor specifically designed to measure the sample chamber conditions at the sensor-gas interface (Appendix B). Figure 13 shows the sensor and sample temperature over time as the chamber is heated from 25°C to 130°C (Figure 13A) and cooled back to 25°C from 130°C (Figure 13B) without air flow (0 mL min^{-1}).

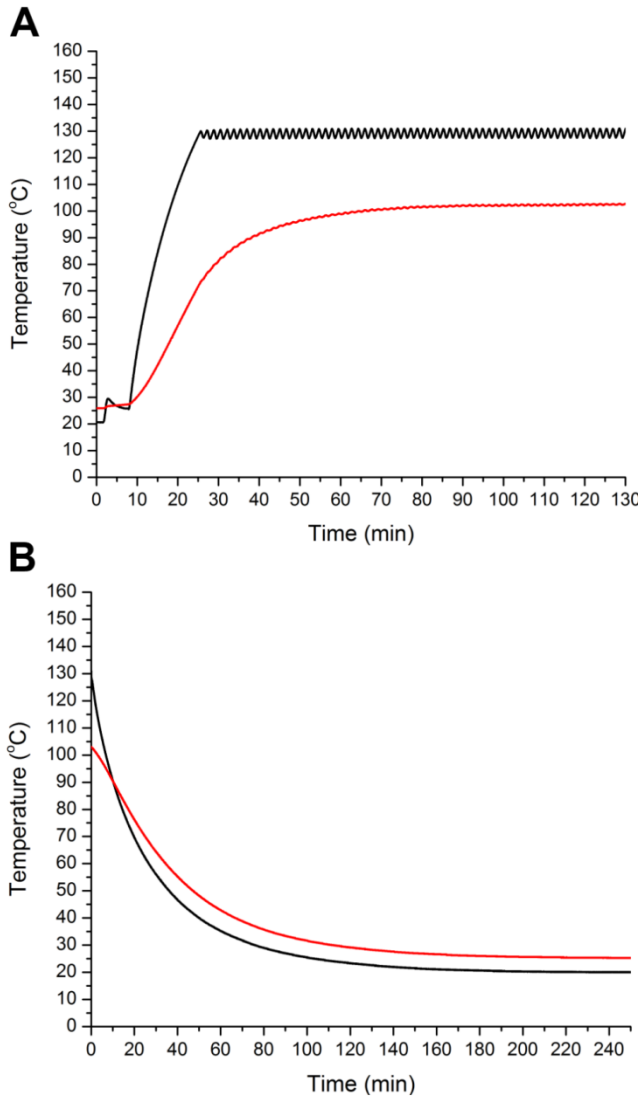

Figure 13: The temperature profile over time without air flow (0 mL min^{-1}) while (A) heating the sample chamber from 25°C to 130°C and (B) cooling the sample chamber from 130°C to 25°C. A custom temperature and relative humidity sensor was used to record the temperature inside the sample chamber (red line) using the Virtual-PGA for electrical connections and a thermocouple placed between the cartridge heaters was used to record the chamber temperature (black line).

The air flow was held constant at 0 mL min^{-1} in Figure 13 to establish a baseline and determine the temperature difference between the chamber wall temperature and the internal, sensor temperature. The chamber wall temperature was held constant at 25°C for 10 minutes then the temperature controller set point was increased to 130°C for Figure 13A. An internal chamber temperature of approximately 100°C was obtained after approximately 40 minutes of heating without air flow, which is 30°C lower than the chamber wall temperature recorded by the thermocouple between the two cartridge heaters. Meanwhile, the chamber wall temperature reaches an equilibrium temperature at approximately 10 minutes. The small oscillation in the chamber wall temperature at equilibrium is a result of the auto-tune procedure for the temperature controller, which uses a PID algorithm and is considered normal behavior by the

manufacturer. The magnitude of the oscillation is relatively small compared to the overall temperature. The initial rise to 30°C in the chamber wall temperature during the first 10 minutes of recording was the result of a software communication issue between the temperature controller and the sample chamber monitoring software. The communication issue was resolved prior to additional characterization.

The cooling of the chamber wall temperature and internal, sensor temperature requires approximately 2 hours for both temperatures to reach an acceptable equilibrium. This is in contrast to the 15 minute time scale for heating the chamber from 25°C to 130°C. The chamber wall temperature cooling rate and internal sensor temperature cooling rate are approximately the same after the first 20 minutes of cooling. There is an initial, fast cooling of the chamber wall temperature for the first 20 minutes as the temperature controller stops actively controlling the temperature. There is no active cooling of the sample chamber, while there are cartridge heaters and a temperature controller to perform active heating. The sample chamber could be cooled faster with an active cooling mechanism, such as liquid nitrogen or a refrigeration recirculation system. Flowing cooler air through the sample chamber would improve the cooling rate as well. Currently, the focus is on maintaining higher temperatures to minimize wall adsorption effects inside the chamber; thus, active cooling mechanisms have not been implemented.

Room temperature (25°C) air was flowed through the sample chamber at various flow rates from 0 to 1000 mL min^{-1}. The results are seen in Figure 14. The sample chamber temperature was heated from 25°C to 130°C. The 1000 mL min^{-1} air flow rate is the maximum flow for the mass flow controller used in conjunction with a vacuum pump to pull room air through the chamber. Figure 14D shows the internal, sensor temperature for all four flow rates tested (0, 100, 500, and 1000 mL min^{-1}) while the chamber wall temperature was increased from 25°C to 130°C. The bottom section of the chamber was left unheated at room temperature. Regardless of flow rate, the equilibrium internal, sensor temperature was consistently 30°C lower than the chamber wall temperature. The small oscillations in the chamber wall temperature were still observed after reaching equilibrium, and are a result of the temperature controller PID algorithm. The equilibrium temperature appears to be independent of flow rate. However, the heating rate is flow-rate dependent as the four plots in Figure 14D do not overlap until reaching an equilibrium temperature within a 5°C range after approximately 1 hour of heating. This result may change if hot or cold air is pulled through the sample chamber instead of room temperature air. The relative humidity, which may influence wall adsorption and chamber temperature, was not recorded during this characterization. A controllable relative humidity source would have to be connected to the sample chamber for a complete study of the influence of temperature and relative humidity on internal chamber conditions.

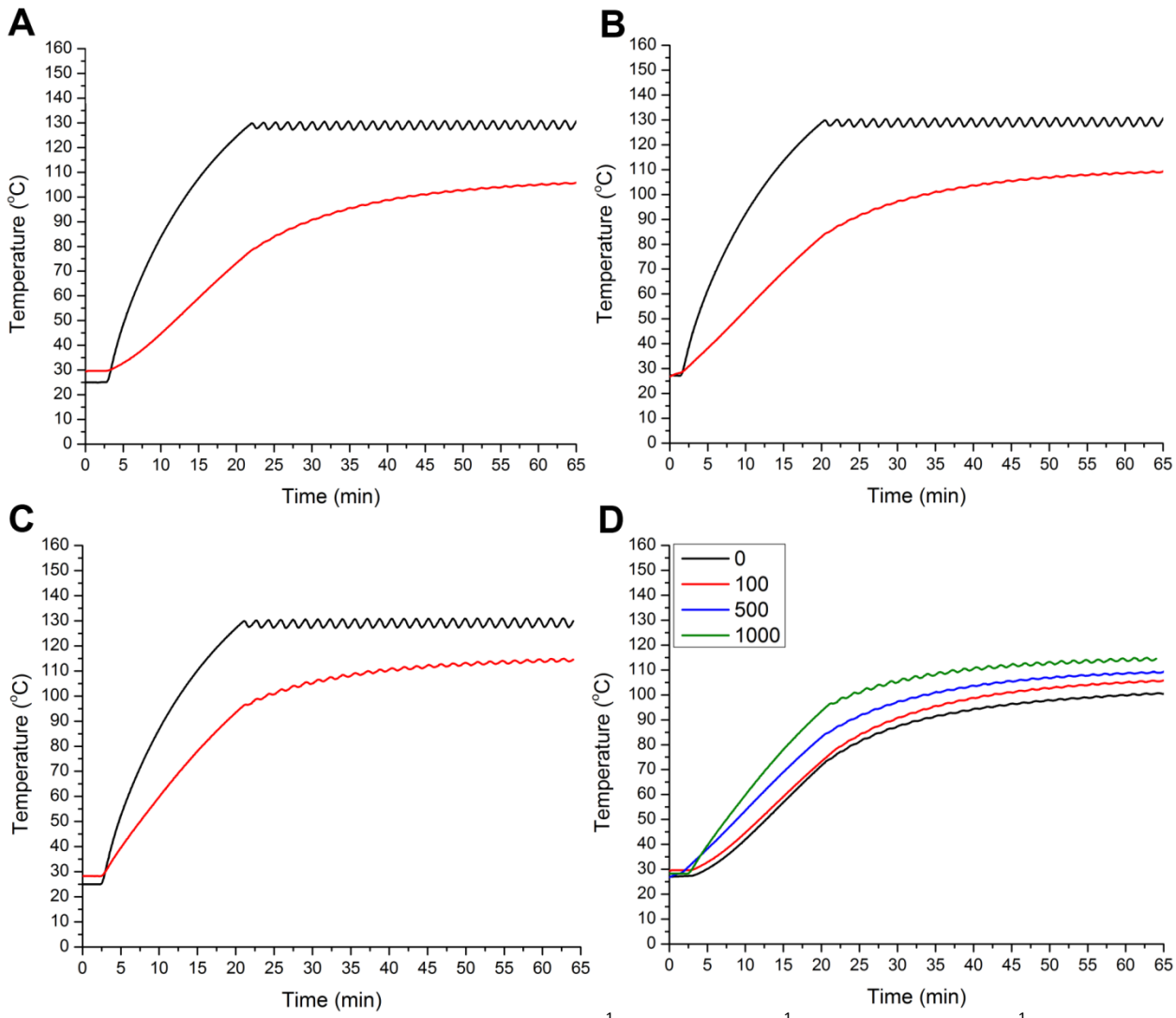

Figure 14: The temperature versus time for (A) 100 mL min^{-1}, (B) 500 mL min^{-1}, and (C) 1000 mL min^{-1} air flow with the chamber wall temperature (black line) and internal, sensor temperature (red line) from 25°C to 130°C. (D) A comparison of the internal, sensor temperature over time while the chamber wall temperature was increased from 25°C to 130°C at different air flow rates (0, 100, 500, and 1000 mL min^{-1}). Room temperature (25°C) air was used as the carrier gas.

VI. Conclusions

A versatile sample chamber for vapor delivery and sensor performance evaluation with a VPGA was assembled. An impactor-inspired, cone geometry was used to uniformly distribute vapor across the entire surface of a sensor. The top section of the sample chamber can be temperature controlled to minimize wall adsorption effects and conduct temperature studies relative to sensor performance. The bottom section utilized off-the-shelf chip carriers and sockets with simple, custom printed circuit boards for rapid loading and unloading of prototype sensors. The socket and circuit board could be removed for larger sensors. To accompany the flexibility of the sample chamber, a VPGA was created using commercially available electronics and in-house software. The patterns associated with each prototype sensor were saved in XML

files, which improved usability and information exchange. A complete system diagram of the sample chamber and VPGA, including the temperature controller, mass flow controller, and vacuum pump is seen in Figure 15. The full system scaled to seven sample chambers could theoretically monitor 448 sensors. In combination with a parallel vapor delivery system, the impactor sample chamber and VPGA system allow for high throughput sensor performance evaluation on an unparalleled scale without additional hardware, electronics, or software.

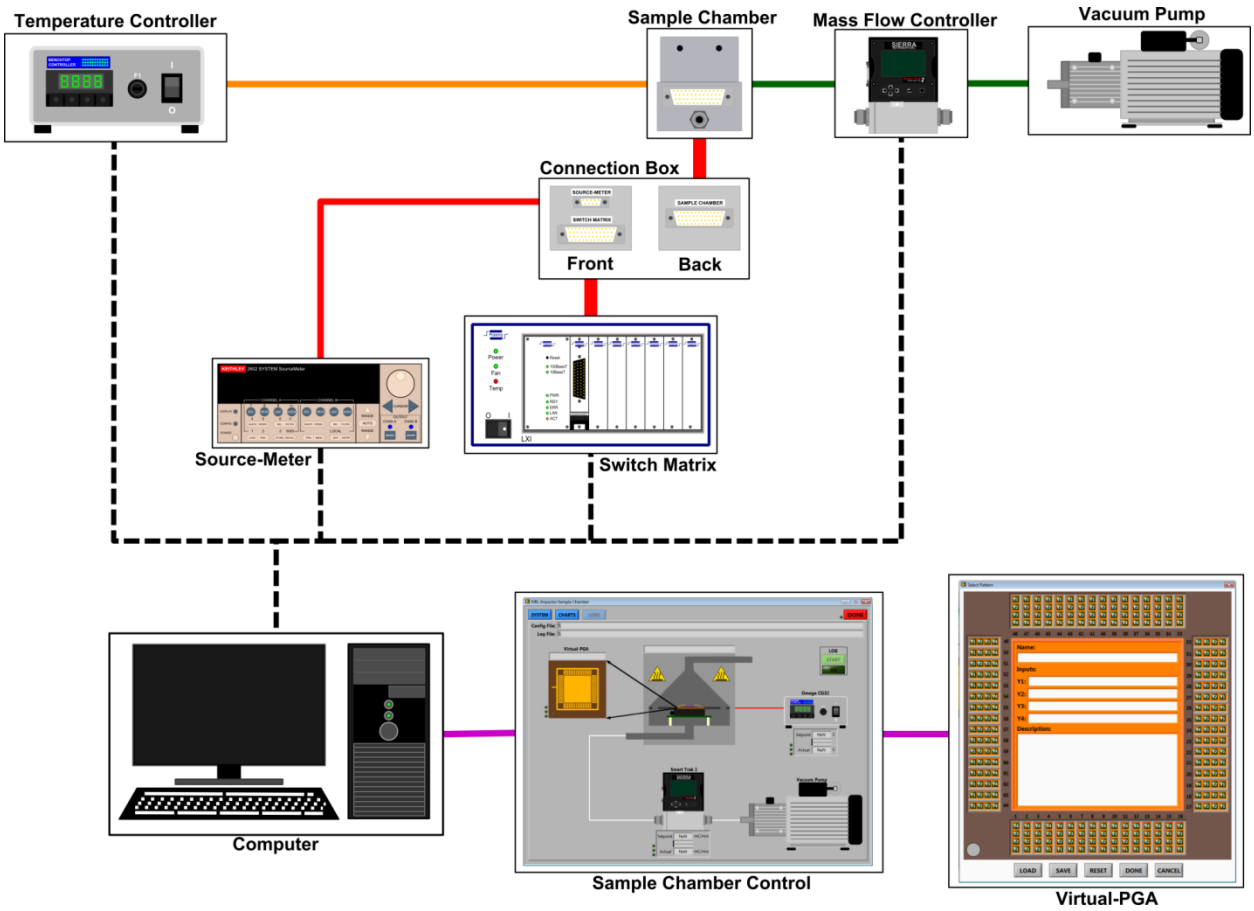

Figure 15: A diagram of all of the components of the impactor sample chamber and Virtual-PGA system. The red lines indicate electrical connections between components for the VPGA. The green lines indicate air flow connections, where vapors are pulled through the sample chamber with a vacuum pump and regulated to a specific flow rate with a mass flow controller, and the orange lines indicate electrical connections for temperature control of the sample chamber. The dashed black lines indicate computer connections for control and monitoring of the system during sensor performance evaluation. The purple lines indicate the software integrated with the computer to monitor and control the VPGA and sample chamber. A single sample chamber configuration can be easily scaled to seven chambers with a multiplexer and additional mass flow controllers.

Acknowledgements

The authors would like to acknowledge Mark Hammond and Greg Collins for their programming advice and help in procuring supplies, respectively. Financial support was provided by the Department of Homeland Security Science and Technology Directorate.

References

[1] S. Singh, Sensors--An effective approach for the detection of explosives, Journal of Hazardous Materials. 144 (2007) 15-28.

[2] P.-C. Chen, F.N. Ishikawa, H.-K. Chang, K. Ryu, C. Zhou, A nanoelectronic nose: a hybrid nanowire/carbon nanotube sensor array with integrated micromachined hotplates for sensitive gas discrimination, Nanotechnology. 20 (2009) 125503.

[3] F. Wang, H. Gu, T.M. Swager, Carbon Nanotube/Polythiophene Chemiresistive Sensors for Chemical Warfare Agents, Journal of the American Chemical Society. 130 (2008) 5392-5393.

[4] J.P. Novak, E.S. Snow, E.J. Houser, D. Park, J.L. Stepnowski, R.A. McGill, Nerve agent detection using networks of single-walled carbon nanotubes, Appl. Phys. Lett. 83 (2003) 4026.

[5] Y. Wang, Z. Zhou, Z. Yang, X. Chen, D. Xu, Y. Zhang, Gas sensors based on deposited single-walled carbon nanotube networks for DMMP detection, Nanotechnology. 20 (2009) 345502.

[6] P.-C. Chen, S. Sukcharoenchoke, K. Ryu, L.G. de Arco, A. Badmaev, C. Wang, et al., 2,4,6-Trinitrotoluene (TNT) Chemical Sensing Based on Aligned Single-Walled Carbon Nanotubes and ZnO Nanowires, Adv. Mater. 22 (2010) 1900-1904.

[7] J.T. Robinson, F.K. Perkins, E.S. Snow, Z. Wei, P.E. Sheehan, Reduced Graphene Oxide Molecular Sensors, Nano Letters. 8 (2008) 3137-3140.

[8] P. G. Datskos, N. V. Lavrik, M. J. Sepaniak, Detection of Explosive Compounds with the Use of Microcantilevers with Nanoporous Coatings, Sensor Letters. 1 (2003) 25-32.

[9] L.A. Pinnaduwage, V. Boiadjiev, J.E. Hawk, T. Thundat, Sensitive detection of plastic explosives with self-assembled monolayer-coated microcantilevers, Appl. Phys. Lett. 83 (2003) 1471-1473.

[10] G. Muralidharan, A. Wig, L.A. Pinnaduwage, D. Hedden, T. Thundat, R.T. Lareau, Adsorption-desorption characteristics of explosive vapors investigated with microcantilevers, Ultramicroscopy. 97 (2003) 433-439.

[11] C.R. Field, J. Yeom, A. Salehi-Khojin, R.I. Masel, Robust fabrication of selective and reversible polymer coated carbon nanotube-based gas sensors, Sensors and Actuators B: Chemical. 148 (2010) 315-322.

[12] Y. Engel, R. Elnathan, A. Pevzner, G. Davidi, E. Flaxer, F. Patolsky, Supersensitive Detection of Explosives by Silicon Nanowire Arrays, Angewandte Chemie International Edition. 49 (2010) 6830-6835.

Appendix A: Circuit Diagrams for the Virtual Pin-Grid Array

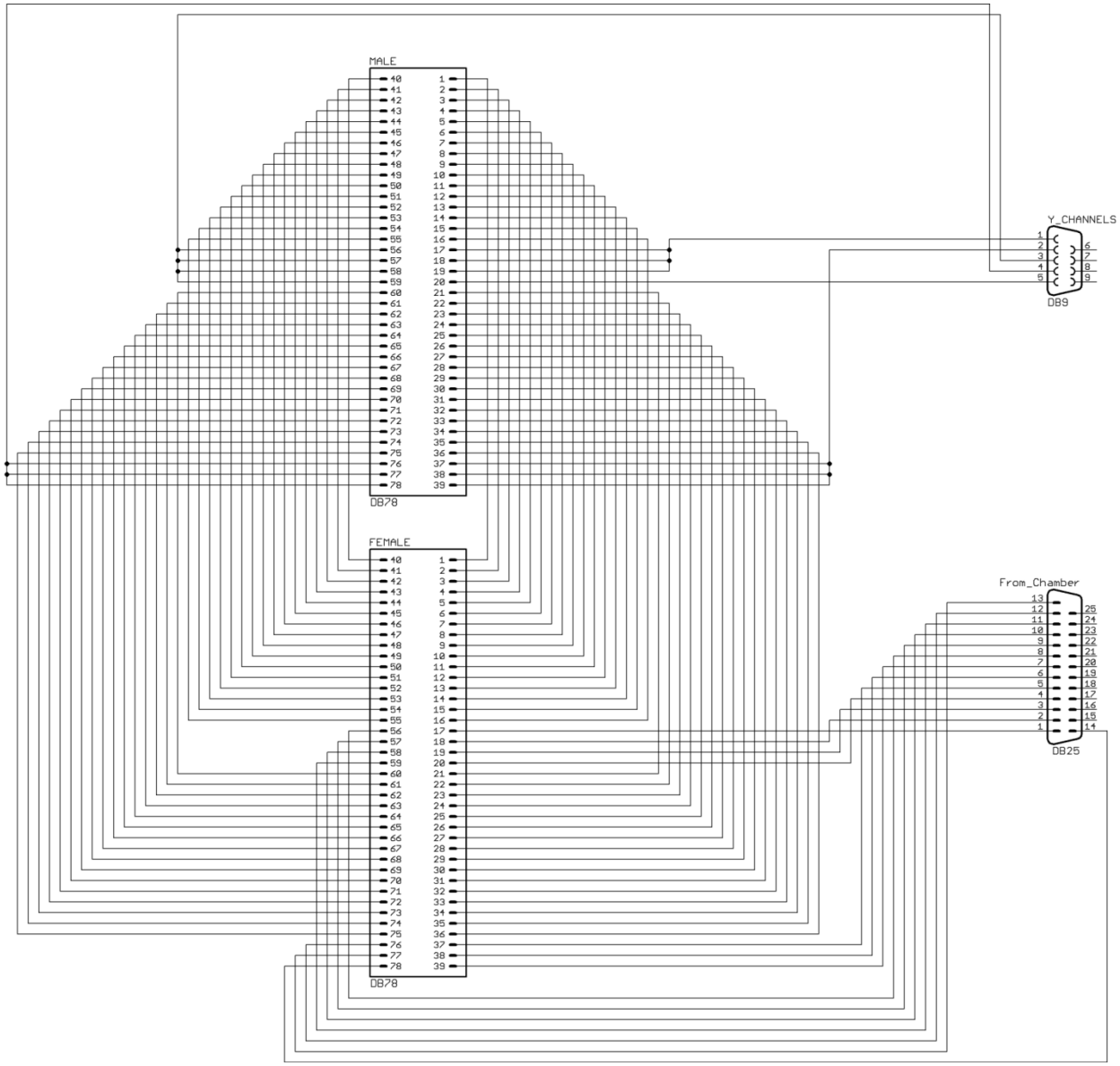

Figure A1: Circuit diagram for the connection box between the 64x4 switch to the impactor-inspired sample chamber

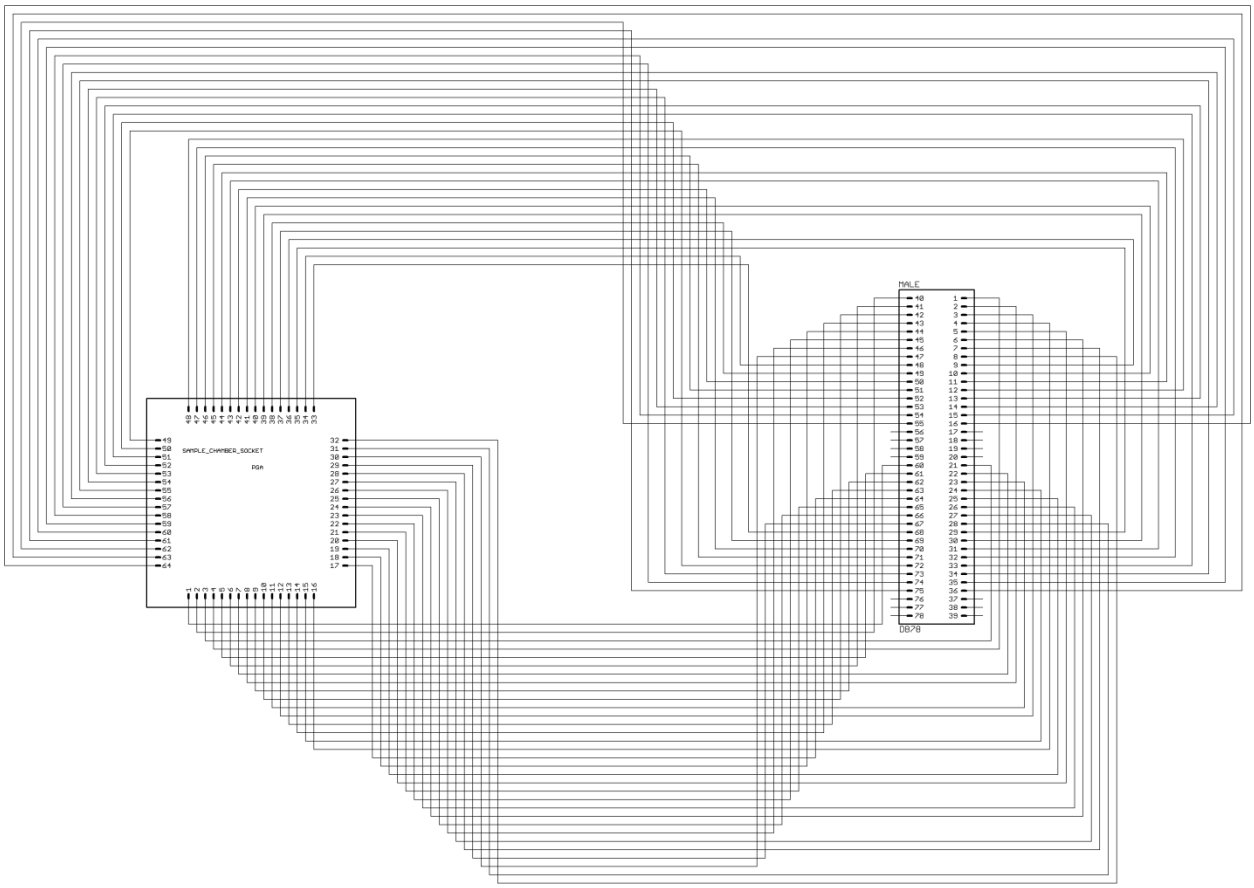

Figure A2: Circuit diagram for the zero-insertion force socket inside the sample chamber to the high-density D-sub 78-pin connector outside the sample chamber.

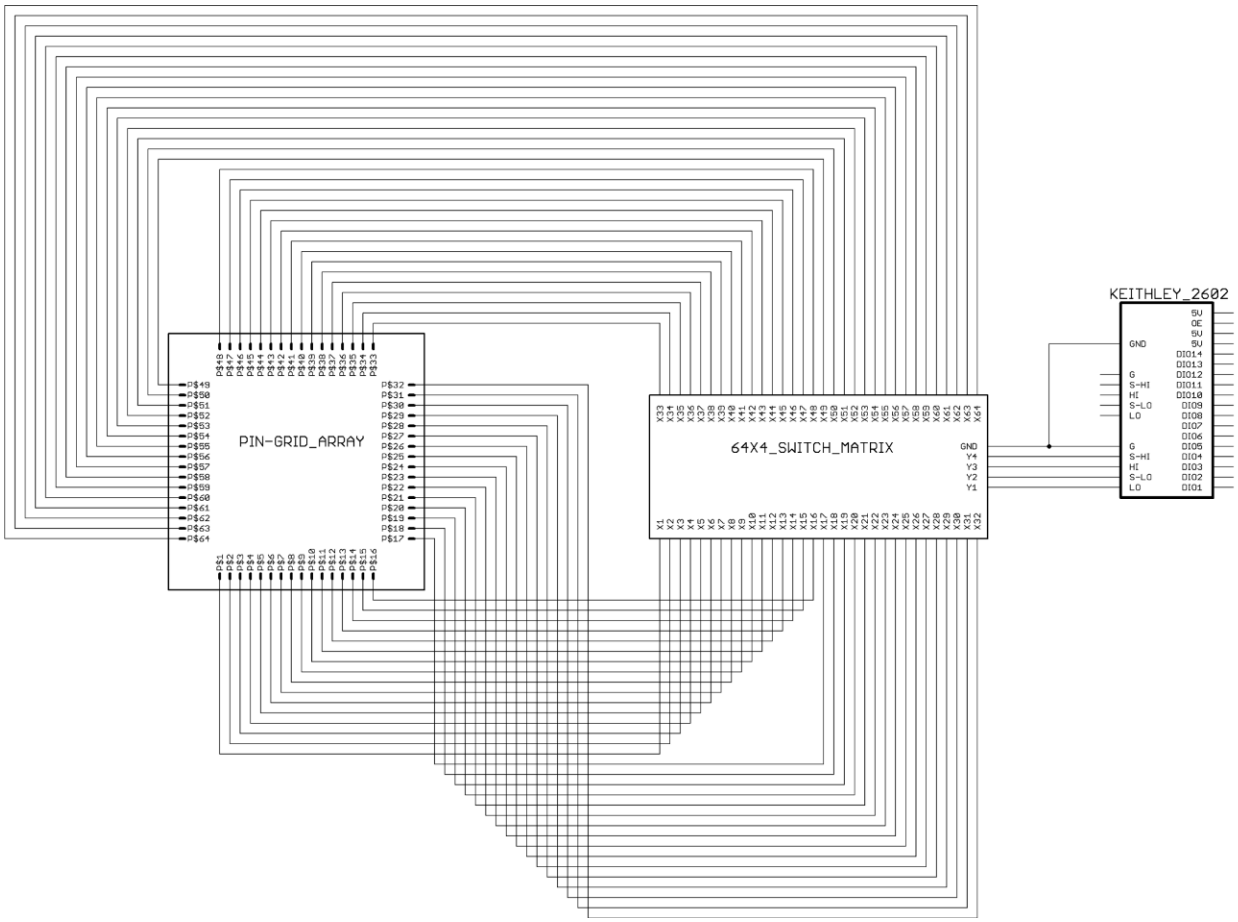

Figure A3: The electrical schematic for the Virtual-PGA hardware. The 64 pins of the pin-grid array are connected to the 64 output, or *X*, channels of the 64x4 switch matrix. The four inputs, or *Y*, channels of the switch matrix are connected to the four output channels of the source-meter: source high (HI), source low (LO), sense high (S-HI), and sense low (S-LO). The chassis ground (GND) of the source-meter is connected to the ground of the output unit (G) and the ground of the switch matrix (GND).

Appendix B: A Custom Temperature and Relative Humidity Sensor

A temperature and relative humidity sensor was assembled to insert into the zero-insertion force (ZIF) socket of the impactor-inspired electronic sample chamber. A Sensirion SHT15 temperature and relative humidity sensor (SHT15, Sensirion AG, Zurich, Switzerland) was mounted on a custom printed circuit board (PCB) that matched the dimensions of the 64-pin pin-grid array (PGA) chip carrier. A circuit diagram is seen in Figure B1, while a placement diagram and image of the PCB are shown in Figure B2. The PCB was designed to have the SHT15 sensor placed directly at the center of the cone of the sample chamber.

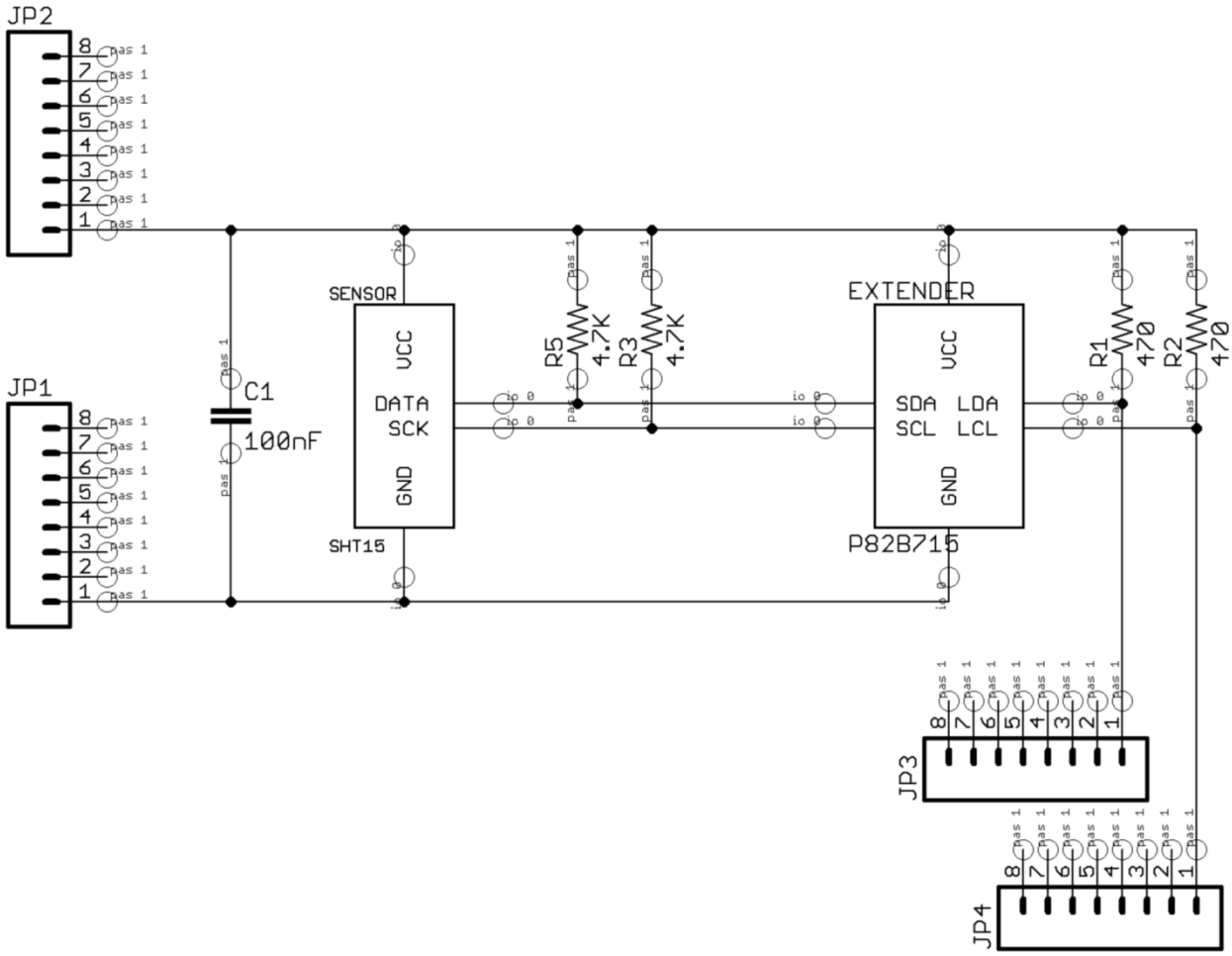

Figure B1: The circuit diagram for the PGA Insert that contains the SHT15 temperature and relative humidity sensor and the I^2C bus extender.

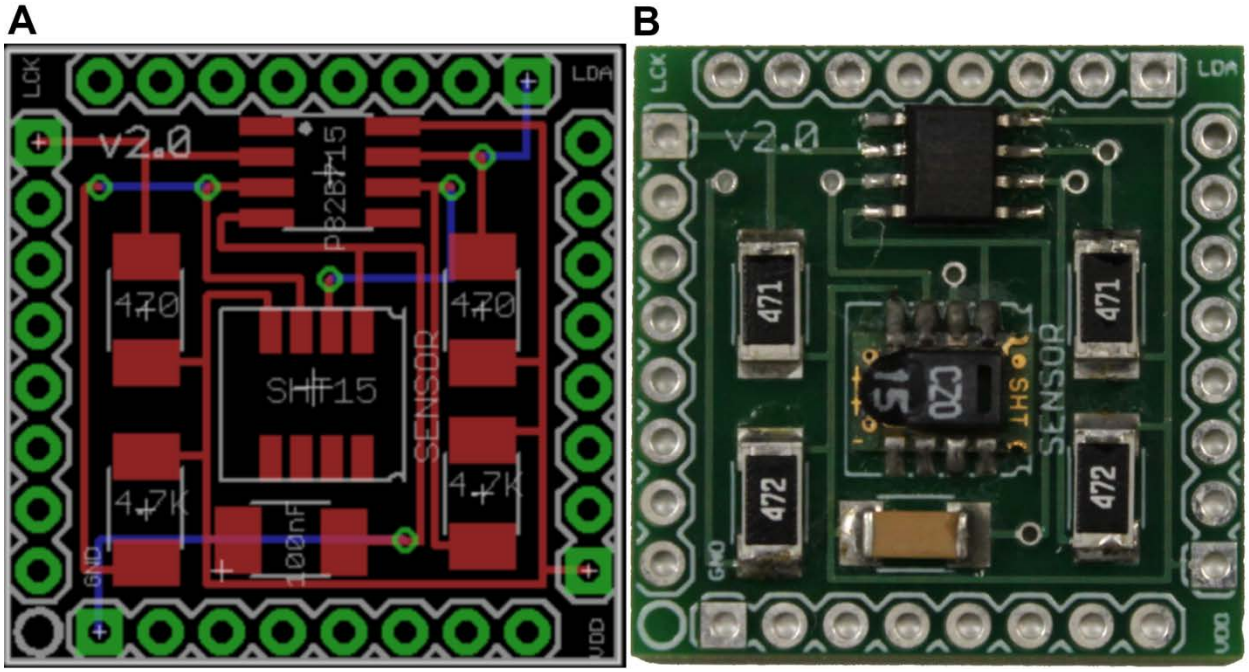

Figure B2: (A) The placement diagram for the PGA Insert with the SHT15 temperature and relative humidity. (B) The printed circuit board with the various components soldered to the board. The PCB is the same size as the PGA and is designed to sit in the zero-insertion force socket of the sample chamber.

The sensor communicates with a microcontroller or computer using the I^2C communication protocol. However, the I^2C protocol only has a usable transmission distance of 10 cm. The 10-cm transmission distance is too short to be used with the Virtual-PGA due to the cable length from the sample chamber to the connection box and from the switch to the read out device. Thus, an I^2C bus extender was incorporated into the circuit to extend the transmission length from 10 cm to theoretically 100 meters. The bus extenders work as a pair, so a second bus extender is incorporated into the sensor read out circuit. Table B1 summarizes the pin connections for the sensor.

Table B1: Pin connections for the SHT15 sensor and I^2C bus extender for the PGA insert printed-circuit board

SHT15 Pin	I^2C Extender Pin	PGA Pin	Function
1	-	3	GND
2	6	35	DATA (LDA)
3	3	51	CLOCK (LCK)
4	-	19	VCC (5V)

A sensor readout device, known as the sensor hub, was created using the Arduino Uno microcontroller. The Arduino Uno (DEV-09950, Sparkfun Electronics, Boulder, Colorado USA) is a well-established open-source “hobbyist” microcontroller, focused on ease-of-use and teaching of embedded control applications. Consequently, there is a vast online community with documentation for the Uno and readily available components for assembling embedded circuits. The Arduino Uno uses an Atmega328 microcontroller with thirteen digital TTL control

lines, six (6) 10-bit resolution 0-5 V analog inputs, TTL serial communication, I^2C serial communication, and an open-source integrated development environment (IDE).

The circuit prototyping and initial evaluation were conducted using an Arduino Uno development board, but the final iteration of the sensor hub only used the Atmega328 microcontroller with the preloaded Optboot (Uno) bootloader (DEV-10524, Sparkfun Electronics, Boulder, Colorado USA). After including the LCD channels, there were enough digital channels to communicate with three sensors via the I^2C protocol with the three bus extenders and provide serial communication with a computer. A MAX233 chip was used to convert the TTL (0 to 5V) signals to a RS-232 signal, which is a bidirectional signal up to 15V. The use of the MAX233 chips allows for communication with the sensor hub via a computer. A liquid crystal display (LCD, LCD-00709, Sparkfun Electronics, Boulder, Colorado USA) is used to display the temperature (C) and relative humidity (%) to the user for up to three connected sensors. If a sensor is not connected to the sensor hub on power up, then the sensor information would not be displayed on the LCD. Figure B3 shows the placement of components in the sensor hub PCB and an image of the assembled board. A circuit diagram of the sensor hub is seen in Figure B4, and a complete parts list is listed in Table B2.

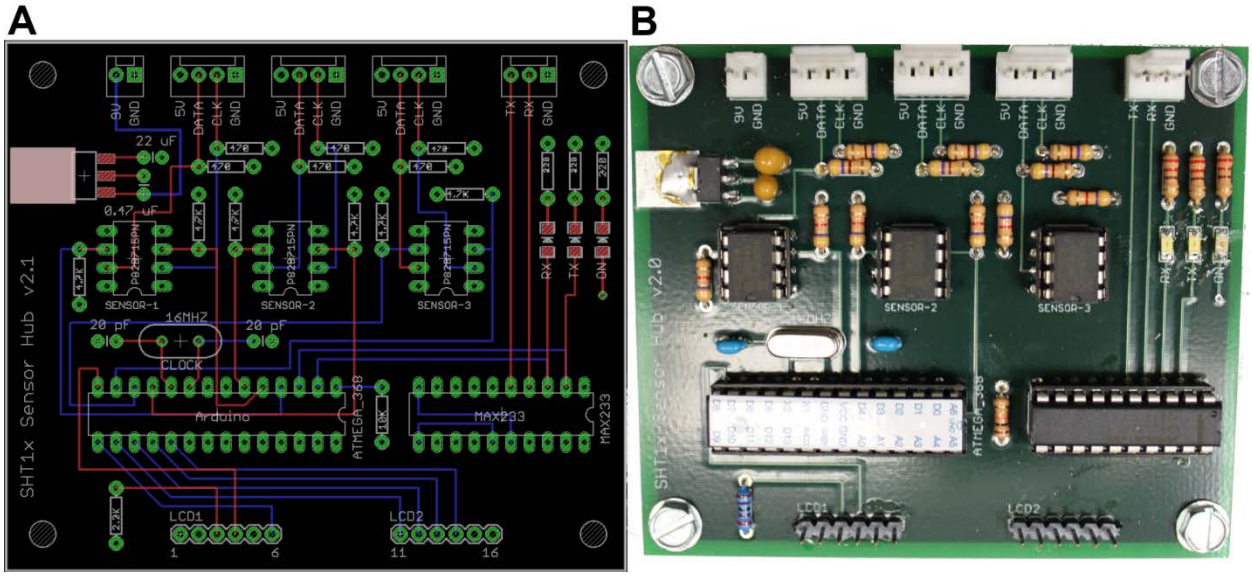

Figure B3: (A) The placement diagram for the sensor hub printed-circuit board (PCB) for the SHT15 temperature and relative humidity sensor. (B) An image of the components mounted and soldered to the PCB.

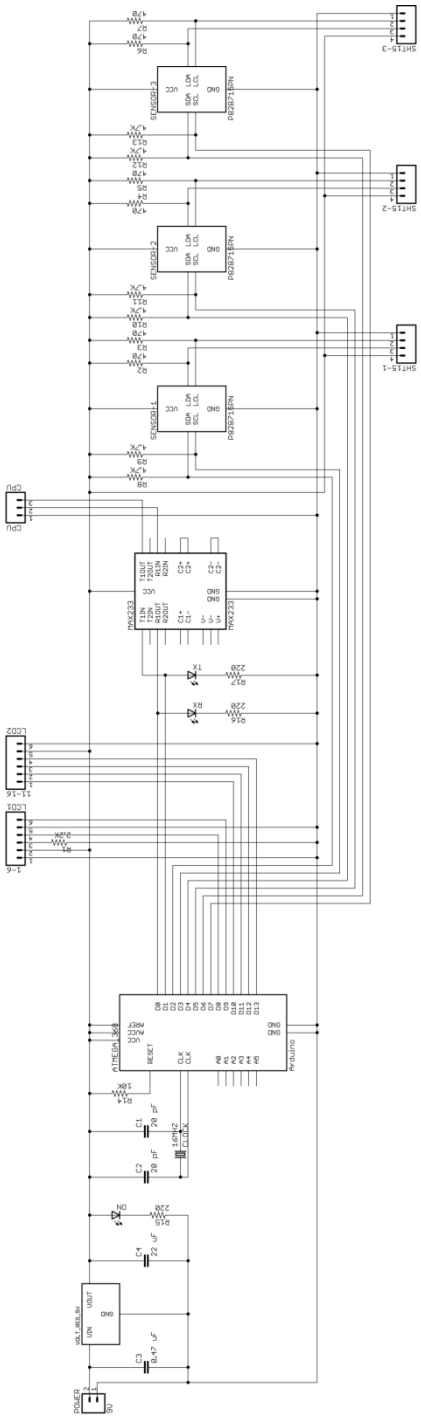

Figure B4: A circuit diagram for the SHT15 temperature and relative humidity sensor hub.

Table B2: A complete parts list for the SHT15 PGA insert and sensor hub electronics.

Part Description	Qty	Part Number	Manufacturer
9V power supply	1	EPS090066-P5P	CUI Inc
Power supply connector	1	PJ-005A	CUI Inc
9V to 5V voltage regulator	1	LM2940-5.0	National Semiconductor
On-Off Toggle Switch SPDT	1	M2011SS1W01/UC	NKK Switches
4-Pin mini-DIN jack	3	MD-40	CUI Inc
4-Pin mini-DIN connector	3	MD-40CV	CUI Inc
Connection housing 3-position with locking ramp	1	09-50-3031	Molex Connector Corporation
Connection housing 4-position with locking ramp	1	09-50-3041	Molex Connector Corporation
Connection terminal female 18-24 AWG Tin	4	08-52-0072	Molex Connector Corporation
Connection housing 4-position with locking ramp 0.100'' spacing	3	22-01-3047	Molex Connector Corporation
Connection housing 3-position with locking ramp 0.100'' spacing	1	22-01-3037	Molex Connector Corporation
Connection housing 2-position with locking ramp 0.100'' spacing	1	22-01-3027	Molex Connector Corporation
Connection header 4-position with friction lock 0.100'' spacing	3	22-27-2041	Molex Connector Corporation
Connection header 3-position with friction lock 0.100'' spacing	1	22-27-2031	Molex Connector Corporation
Connection header 2-position with friction lock 0.100'' spacing	1	22-27-2021	Molex Connector Corporation
Connection terminal female 22-30 AWG Tin	17	08-50-0114	Molex Connector Corporation
470 Ohm SMD Resistor	2	ERJ-12ZYJ471U	Panasonic - ECG
4.7K Ohm SMD Resistor	2	ERJ-12ZYJ472U	Panasonic - ECG
470 Ohm Through hole Resistor	6	CFR-25JB-470R	Yageo
4.7K Ohm Through hole Resistor	6	CFR-25JB-4K7	Yageo
2.2K Ohm Through hole Resistor	1	MFR-25FBF-2K10	Yageo
220 Ohm Through hole Resistor	1	CFR-25JB-220R	Yageo
10K Ohm Through hole Resistor	1	CFR-25JB-10K	Yageo
16 MHz Oscillator	1	ECS-160-20-4X	ECS Inc
20 pF Through hole Capacitor	2	RPE5C2A200J2P1Z03B	Murata Electronics North America
22 uF Capacitor	2	T350D226K006AT	Kemet
0.47 uF Capacitor	2	T350B474K050AT	Kemet
100nF SMD Capacitor	1	GRM155F51C104ZA01D	Murata Electronics North America
8x1 Header Pins	4	68001-436HLF	FCI
LED SMD-1206	1	CMDA1CG7A1Z	Chicago Miniature Lighting
Yellow LED SMD-1206	2	CMD15-21VYD/TR8	Chicago Miniature Lighting
Temperature and Relative Humidity Sensor	1	SHT15	Sensirion
RS232-to-TTL chip	1	MAX233CPP	Maxim
IC I2C Bus Extender 8-SOIC	1	P82B715TD,112	NXP Semiconductors
IC I2C Bus Extender 8-DIP	3	P82B715TD,112	NXP Semiconductors
DB9 Connector Male	1	5-747904-5	TE Connectivity
Microcontroller	1	ATmega328	Atmel
White on Black LCD Display	1	GDM1602K	Xiamen Ocular
8-pin DIP Socket	3	1-390261-2	TE Connectivity

20-pin DIP Socket	1	2-641612-1	TE Connectivity
28-pin DIP Socket	1	1-390261-9	TE Connectivity
Plastic project box	1	1598BSGY	Hammond Manufacturing

A shielded four channel cable, two pair independently shielded, was made with a DB9 connector and a circular PS-2 4-pin (S-Video) connector to connect the sensor hub to the Virtual-PGA connection box. Table B3 summarizes the cable and connector pin connections. The sensor hub is capable of monitoring and recording the temperature and relative humidity from three SHT15 sensors, as long as I^2C bus extenders have been added to the circuit. Currently, there is no option to bypass the bus extenders.

Table B3: Pin connections for the circular PS-2 connector (S-Video) used to make connection from the SHT1x sensor hub to the Virtual-PGA with a DB9 connector. The PS-2 pins are numbered clockwise, starting in the lower left hand corner.

PS-2 4 Pin Connector	DB9 Connector	Function
1	3	5V
2	2	LCL
3	1	GND
4	4	LDA

The sensor hub displays on the LCD screen only the temperature and relative humidity of sensors connected to the hub. The LCD screen cycles through all connected sensors, and in the case of characterizing the sample chamber, only the temperature and relative humidity for sensor 1 are displayed. The commands and a brief description are seen in Table B4.

TableB4: Summary of commands recognized by the NRL-SHT1x using a 9600 baud rate, 8 bits, 1 stop bit, no parity, and no hardware flow control. All commands must be terminated with a new line character ("\n") and all responses are terminated by a new line character.

Command	Description
T1?	Gets the temperature in Celsius for the SHT1x sensor connected to port 1.
T2?	Gets the temperature in Celsius for the SHT1x sensor connected to port 2.
T3?	Gets the temperature in Celsius for the SHT1x sensor connected to port 3.
R1?	Gets the relative humidity in percent for the SHT1x sensor connected to port 1.
R2?	Gets the relative humidity in percent for the SHT1x sensor connected to port 2.
R3?	Gets the relative humidity in percent for the SHT1x sensor connected to port 3.

A LabVIEW program was written to record the temperature and relative humidity though the sensor hub using the commands outlined in Table. The LabVIEW program and the source code for the microcontroller are provided without warranty on the included CD.

SEE ATTACHED CD FOR PROGRAM AND SOURCE CODE.

Appendix C: The Computer-Aided Design (CAD) files for the Impactor Sample Chamber

The computer design files are provided without warranty. These files can be used to manufacture impactor-inspired sample chambers. The files were generated using AutoDesk Investor.

SEE ATTACHED CD FOR DESIGN FILES.

Appendix D: Source code for the Virtual-PGA and Data Acquisition Software

The source code is provided without warranty. This version of the code does not support multiple sample chambers or a multiplexer. The code is divided into two sections: the Virtual-PGA library and the Data Logging application for the source meter. The code is written in LabVIEW 2010 SP 1 and requires the LabVIEW 2010 run-time engine.

SEE ATTACHED CD FOR PROGRAM AND SOURCE CODE.